bioRxiv preprint doi: https://doi.org/10.1101/407544; this version posted January 15, 2019. The copyright holder for this preprint (which was not certified by peer review) is the author/funder. All rights reserved. No reuse allowed without permission.

The human default consciousness and its disruption: insights from an EEG study of Buddhist jhāna meditation

Paul Dennison*

Correspondence:
pd@pauldennisonpsychotherapy.co.uk

The "neural correlates of consciousness" (NCC) is a familiar topic in neuroscience, overlapping with research on the brain's "default mode network". Task-based studies of NCC by their nature recruit one part of the cortical network to study another, and are therefore both limited and compromised in what they can reveal about consciousness itself. The form of consciousness explored in such research, we term the human default consciousness (DCs), our everyday waking consciousness. In contrast, studies of anaesthesia, coma, deep sleep, or some extreme pathological states such as epilepsy, reveal very different cortical activity; all of which states are essentially involuntary, and generally regarded as "unconscious". An exception to involuntary disruption of consciousness is Buddhist jhāna meditation, whose implicit aim is to intentionally withdraw from the default consciousness, to an inward-directed state of stillness referred to as jhāna consciousness, as a basis to develop insight. The default consciousness is sensorily-based, where information about, and our experience of, the outer world is evaluated against personal and organic needs and forms the basis of our ongoing self-experience. This view conforms both to Buddhist models, and to the emerging work on active inference and minimisation of free energy in determining the network balance of the human default consciousness.

This paper is a preliminary report on the first detailed EEG study of jhāna meditation, with findings radically different to studies of more familiar, less focused forms of meditation. While remaining highly alert and "present" in their subjective experience, a high proportion of subjects display "spindle" activity in their EEG, superficially similar to sleep spindles of stage 2 nREM sleep, while more-experienced subjects display high voltage slow-waves reminiscent, but significantly different, to the slow waves of deeper stage 4 nREM sleep, or even high-voltage delta coma. Some others show brief posterior spike-wave bursts, again similar, but with significant differences, to absence epilepsy. Some subjects also develop the ability to consciously evoke clonic seizure-like activity at will, under full control. We suggest that the remarkable nature of these observations reflects a profound disruption of the human DCs when the personal element is progressively withdrawn.

Keywords: EEG, meditation, jhāna, consciousness, epilepsy, slow-waves, spike-waves

Abstract 347 words
Main text 11734 words

bioRxiv preprint doi: https://doi.org/10.1101/407544; this version posted January 15, 2019. The copyright holder for this preprint (which was not certified by peer review) is the author/funder. All rights reserved. No reuse allowed without permission.

1. INTRODUCTION

1.1. A DEFAULT SENSORY CONSCIOUSNESS (DCs)

We consider the DCs to be a sensory consciousness, irrespective of whether we are responding to direct sensory input, accessing memory or processing ideas, or indeed dreaming, all of which are experienced within a sensory framework. This consciousness is represented at the cortical and biological level as an ongoing dynamic functional organisation intrinsic to our lives as human beings interacting with others and the world. This default consciousness is the *de facto* subject of the many "content" studies of neural correlates of consciousness (NCC) where researchers examine which cortical networks are stimulated or suppressed by a subject undergoing tasks or external stimuli (Koch *et al*., 2016; Boly *et al*., 2017).

A subjective component is ever-present in the DCs, and is likely the dominant factor in the dynamic neuronal balance between inputs from the outer world and from our body, with their resonances to past experiences held in memory, then weighed as to their value to the "I" or "self" in the light of current needs or actions. This understanding of consciousness is implicit in psychoanalysis, from the early work of Freud (1895) in his *Project for a Scientific Psychology*, to the long-established clinical experience of psychotherapists and psychoanalysts of the constant ongoing resonance between current experience and stored memories, particularly memories of reciprocal roles that contain information on the emotional impact of events (pain-pleasure; liking-disliking) for the self (e.g. Ryle and Kerr, 2002; and Matte Blanco's, 1980, description of the *Unconscious as Infinite Sets*). It also conforms to the emerging work within neuroscience on active inference (Friston *et al*., 2016).

Whilst content studies of the NCC can reveal different features of the DCs, state-based approaches compare it to states such as sleep, anaesthesia, coma, epilepsy and some pathological states, mostly regarded as unconscious. If it is possible, as we aim to demonstrate, for a person to intentionally and progressively withdraw their personal involvement from the DCs, even partially, while remaining fully conscious, a new window is opened into exploring the NCC (Hohwy, 2009), and consciousness itself.

1.2. JHĀNA MEDITATION

Given the rather remarkable observations we describe, certainly atypical compared to previous EEG studies of meditation, it is appropriate to give a context and overview of some of the key features of Buddhist jhāna meditation.

Whether Southeast Asian, Tibetan, Japanese or Chinese, Buddhist meditation comprises two strands, Samatha (Wallace, 1999) and Vipassanā (Cousins, 1994-96); the former often translated as tranquillity or serenity, and the latter as insight or wisdom. Mindfulness, though well-known as a form of practice in its own right, and accepted as useful in the treatment of recurrent depression, is just one of the basic factors underpinning both samatha and vipassanā. Jhāna meditation falls within the samatha division. Etymologically, jhāna is often translated as "absorption", but has a secondary root, *jhapeti*, meaning to burn up, which is a reflection that it is a highly active, and far from passive, state (Cousins, 1973; Gunaratana, 1980). While there have been many EEG studies of meditation (Thomas and Cohen, 2014; Cahn and Polich, 2006), there have been no in-depth studies of jhāna meditation, and there exist very few centres that teach its practice. The background to this requires some explanation. In South and Southeast Asia during the 1950s, Buddhist practices underwent a "Reform", where age-old samatha practices were criticised as unscientific, and repressed in favour of a heavily politically-promoted form of meditation known as Burmese vipassanā, which claimed that jhāna was not necessary as a prerequisite for insight and realisation of Buddhist goals (Crosby, 2013). As a result, jhāna meditation was relegated to an almost esoteric role, sidelined in favour of vipassanā. Many also believed it was not possible to develop and practice jhāna in a lay context, outside monastic and forest meditation traditions.

Recently, an interest in jhāna has revived, with two main traditions emerging in the West. The first, and best known, comes via monastic teachers, and in this form the breath is not controlled in a formal manner. Hagerty *et al.* (2013) describe an EEG study of a single Western practitioner of this method, but with results very different to those we find. In the second form, the length of breath *is* controlled in the

bioRxiv preprint doi: https://doi.org/10.1101/407544; this version posted January 15, 2019. The copyright holder for this preprint (which was not certified by peer review) is the author/funder. All rights reserved. No reuse allowed without permission.

approach to jhāna, since the "normal" length is regarded as integral to the DCs, withdrawal from which is the primary aim of jhāna. This form was introduced to the UK in the 1960s by a former Thai-Cambodian Buddhist monk (The Samatha Trust, UK regd Charity 1973), and is closely related to the *Yogāvacara*, a formerly widespread and ancient, mainly oral, tradition of meditation, practiced by both monks and lay people across South and Southeast Asia, currently the subject of research by ethnologists based on palm-leaf manuscripts discovered in Cambodia and Thailand (Bizot, 1994; Crosby, 2000). In some monasteries, *Yogāvacara* techniques were regarded as a means to develop mastery of jhāna, but were also considered particularly suitable for lay meditators leading normal household lives, as are the subjects of this study. Using lengths of breath longer or shorter than "normal", marks a protected space where jhāna can be safely developed, and safely left to return to the normal DCs and daily life without conflict. "Safely", refers to the containment of highly energised states frequently developed in approaching jhāna; in this respect, and in the precise ways in which the breath is controlled, there are similarities to Tibetan Buddhist yoga (Minvaleev, 2014).

Wallace (1999), referring to the samatha tradition and the practice of jhāna, comments that "The mind and consciousness itself are the primary subjects of introspective investigation within the Buddhist tradition". Indeed, the techniques employed are remarkably relevant to current neuroscience, once the different terminologies are understood. To develop jhāna, the meditator's first task is to overcome the "hindrances", usually listed as: sense-desire, ill-will, sloth and torpor, restlessness and worry, and doubt (Cousins, 1973; Gunaratana, 1980). These represent, in our terms, key features of the human DCs: a constant evaluation of sensory input against past experience and future needs and expectations, based on value to the "I" or "self", which implies liking or disliking, pleasure versus pain, habits of attachment, as well as available energy, restlessness and doubt. In practice, a meditator does not think about or dwell on the hindrances during meditation, but simply begins by turning attention to the breath; each time the mind wanders, distractions in the form of thoughts or feelings are acknowledged and attention patiently, again and again, brought back to the breath. The Buddhist jhāna tradition describes eight jhānas: four rūpa (form) jhānas, and four arūpa (formless) jhānas; of which this paper deals with the former.

1.2.1. Attention

The jhānas are described by their characterising factors; 5 factors for the first rūpa jhāna, 3 for the second, and 2 for the third and fourth jhānas, as listed below with the Pali terms:

First rūpa jhāna factors
- Applied attention, or initial thought (= *vitakka*)
- Sustained attention or thought (= *vicāra*)
- Energised interest, or "joy" (= *pīti*)
- Happiness, contentment or bliss (= *sukha*)
- One-pointedness of mind (= *ekaggatācitta*)

Second rūpa jhāna factors
- Energised interest, or "joy" (= *pīti*)
- Happiness, contentment or bliss (= *sukha*)
- One-pointedness of mind (= *ekaggatācitta*)

Third rūpa jhāna factors
- Happiness, contentment or bliss (= *sukha*)
- One-pointedness of mind (= *ekaggatācitta*)

Fourth rūpa jhāna factors
- One-pointedness of mind (= *ekaggatācitta*)
- Equanimity(= *upekkha*)

The jhānas are a progressive sequence towards deeper states of equanimity, or serenity. The dominant factors of the first rūpa jhāna are two aspects of attention: *vitakka*, applied attention, is the repeated placing of attention on the meditation object, in this case the breath; and *vicāra*, sustained attention, develops as the meditator becomes more skilled at noticing and resisting distraction. Once attention is stabilised internally, the meditator can progress towards the second, third and fourth jhānas, which are

bioRxiv preprint doi: https://doi.org/10.1101/407544; this version posted January 15, 2019. The copyright holder for this preprint (which was not certified by peer review) is the author/funder. All rights reserved. No reuse allowed without permission.

more feeling-based, and share an increasing sense of equanimity. Working with attention is the dominant activity in developing the first jhāna, and is required to be developed to a high level, often over years of practice. Typically practitioners start by mentally counting during in and out breaths, to aid noticing when attention wanders. Distractions are acknowledged minimally, before returning to the count. Maintaining different lengths of breath aids mindfulness, and four lengths are used, two longer than "normal", and two shorter. As distraction eases, counting is dropped, replaced by following the breath from its touch at the nose tip, through the sensations at the throat, chest and diaphragm, and back on the out-breath; noting and managing distractions. This phase is described as developing access concentration. Finally the meditator rests attention at one point, usually the nose tip, and at this stage attention is progressively transferred to an internal mental object, referred to in the jhāna texts as the *nimitta* (Wallace, 1999; Cousins, 1973) or "sign", which is the meditator's growing sense of his/her own consciousness. We are tempted to say the "qualia" of that consciousness, provided qualia is not interpreted in sensory terms as too-crudely "this" or "that".

Allowing for terminology, we expect these two factors of attention to have counterparts in the executive attention networks of the brain. However, attention is inseparable from broader processes of perception (Hohwy 2012), which requires us to consider the personal component, and the subjective experience of the meditator is a clue as to what we might expect. At first a meditator's attention, as in the DCs, is strongly sensorily-determined by the habit or need to mentally "commentate", "name" or "recognise", i.e. to orient experience within the familiar sensory structure of the DCs. Since subjectivity in these perceptual processes is heavily "Eye/I"-driven, we may expect disruption to the executive attention networks, but also to the ventral and dorsal perceptual streams (Milner, 2017; Cloutman, 2012), as the meditator resists the pull back towards DCs processes in developing the first rūpa jhāna.

1.2.2. Attachment

Development of the second, third and fourth rūpa jhānas is more concerned with feeling, and the underlying subject-object nature of consciousness rather than the cognitive processes of attention. In fact, even to develop the first rūpa jhāna, meditators are already working with resisting attachment to liking and disliking, which in Buddhist terms are the roots of craving and the source of suffering. Here there is a correspondence to Freud's "pleasure principle", and the twin pulls of craving and aversion, as well as the importance of understanding attachment disorders in psychiatry and psychotherapy. Since liking and disliking, and associated emotions, are dominant features of our habitual DCs, linking perception to action choices, it may be no surprise to find rather dramatic changes in brain activity when the personal element is withdrawn from the DCs.

Subjectively, the movement from the first to the second rūpa jhāna is characterised by a growing sense of peace and contentment, at the increasing freedom from dependence on DCs processes, as well as a growing "energised interest". These are the two factors *sukha* and *pīti*, respectively, listed above for the second rūpa jhāna, together with the third factor one-pointedness of mind (*ekaggatācitta*) which underpins all four jhānas. The factor *pīti* is strongly emphasised in the Yogāvacara, which lists 5 levels of intensity ranging from fine bodily vibration or prickling of the hairs on the head and body, to, at its most intense, bodily shaking and even jumping in the air (*The Yogāvachara's Manual*). *Pīti* represents the growing involvement of the body and subtle bodily energies into a state of mind-body integration referred to as *samādhi*, a term frequently used interchangeably with "concentration" or jhāna. The EEG observations of high energy states described in this paper, are, we believe, the counterparts of this energisation, and signal the beginnings of a transition to the second and higher rūpa jhānas.

1.2.3. Subject-Object

Whilst the task of the first rūpa jhāna is to develop a degree of mastery of attention, the task of the second rūpa jhāna is to master *pīti*; not to suppress it, but to tranquilise (pali, *passaddhi*) any bodily disturbance into an increasingly still mental state "held" by attention to the *nimitta*. For some meditators the *nimitta* is experienced visually as light, for others as touching something intangible with the mind, or by others as listening to silence (Buddhaghosa, *Visuddhimagga*); these differing experiences reflecting

bioRxiv preprint doi: https://doi.org/10.1101/407544; this version posted January 15, 2019. The copyright holder for this preprint (which was not certified by peer review) is the author/funder. All rights reserved. No reuse allowed without permission.

the traces of a meditator's habitual preference for one or other sense modality in their DCs. Once *pīti* is tranquilised and incorporated, the third rūpa jhāna can develop, and is described in 5th-century texts as being "completely conscious" (Upatissa, *Vimuttimagga*), or with "full awareness like that of a man on a razor's edge" (Buddhaghosa, *Visuddhimagga*). Interestingly, avoiding the words conscious or aware, subjects of this study prefer, "presence", or "vivid presence" for their subjective experience.

Practice of the second, third and fourth rūpa jhānas is also regarded as a progressive exploration and refinement of the subject-object relationship (*nāma-rūpa*, or name and form in Buddhist terms), which becomes less cognitively and sensorily-determined, and less dependent on liking or disliking; such that in the fourth rūpa jhāna even dependence on the "reward" of pleasure or satisfaction ends, replaced by deep stillness and finely poised balance and equanimity. The nature of the subject-object experience is of considerable interest to neuroscience, and will be taken up later in this paper.

However, to develop the jhāna factors is not a straightforward cognitive process, as in task-based EEG studies; meditators cannot simply "think" themselves into jhāna. While the motivation is to withdraw from the habitual DCs ("*secluded from sense desire…*", Cousins, 1973), it is the *nimitta* acting as an "attractor" that allows meditators to settle into jhāna. It could be said that the *nimitta* plays a similar role to the feedback sign in neurofeedback (Sitaram R. *et al*., 2017), and that Samatha meditation is a naturalistic form of neurofeedback, predating modern forms by over two millenia (Dennison, 2012).

2. METHODS AND MATERIALS

2.1. SUBJECTS AND RECORDING PROTOCOL

It is important to acknowledge that meditators in this study, while very experienced in Samatha meditation, vary considerably in their experience of jhāna. Many see jhāna as a progressive process to develop a solid base of equanimity prior to developing insight (vipassanā), and not all are overly concerned to develop mastery of the subtleties between the different jhānas, while leading busy day-to-day lives. In fact none of our subjects would claim complete mastery of jhāna, not surprising given that such mastery is regarded as a rare achievement in Buddhism, described in the 5th century *Visuddhimagga* as of three levels, inferior, medium and superior. In a pilot study in 2010-14, we did not find unequivocal EEG signatures of the different jhānas based on subjective feedback, despite finding startling EEG activity suggesting this form of meditation has profound effects on brain activity. Accordingly, while valuing meditators' subjective feedback, we choose here not to rely primarily on subjective views as to which jhāna meditators feel they are experiencing, but focus rather on the themes of EEG activity that emerge across this broad group of meditators as they attempt to develop ever-deeper stages of jhāna. We then take a cross-discipline approach to compare the EEG evidence with the detailed Buddhist descriptions of the characteristics of the different rūpa jhānas.

Accordingly, we adopt a common protocol for all meditators, using verbal cues to first record a few minutes of resting state eyes-closed and eyes-open EEG, followed by meditators attempting to progressively develop the jhānas, for a total recording time of 35-40 mins. For some meditators this protocol is quicker than their everyday practice, with corresponding disadvantages, but is adopted for consistency. In this way, notwithstanding different levels of skill and pace meditators are capable of in moving through the stages, we look for themes which we then examine against the textual descriptions of the different jhānas. Subjects practice seated on the ground, usually on a cushion, with the body erect and composed, without resting on any supports. The observer/researcher notes events such as shifts in posture, a cough, external noise, or anything likely to cause an artefact.

This is a within-group study, where the control group is, in effect, the wealth of other EEG studies of meditation and the NCC. Twenty-nine experienced meditators from a total pool of around 400 in the UK, Ireland and the US, all experienced in samatha meditation as taught by the Samatha Trust, a UK registered charitable organisation, were recorded during 2014-18, some also re-recorded after 1-3 year intervals. Years' experience of samatha meditation range from 4–40+ years, with most individuals maintaining a daily practise of 30-60 mins, with more intensive 7-10 days "retreats" every 1–3 years.

bioRxiv preprint doi: https://doi.org/10.1101/407544; this version posted January 15, 2019. The copyright holder for this preprint (which was not certified by peer review) is the author/funder. All rights reserved. No reuse allowed without permission.

Twenty-four of the subjects are of graduate or postgraduate-levels of education, and more than half hold, or have held, senior professional roles in health-care or education. Four have spent temporary periods from 1-10 months as ordained Buddhist monks in Thailand. Jhāna practice in detail has been taught and explored by the Samatha Trust only during the last 10 years, and within the group of 29, experience of jhāna varies considerably.

Given that recordings show features superficially similar to deep sleep, it is important to stress that subjects are fully conscious throughout. There are no signs of loss of muscle tone or sleepiness in posture; subjects respond immediately to verbal cues; and at the end show no signs of sleep inertia or disorientation. On the contrary, meditators describe feeling more alert and present during and after practice. The protocol at the end of a recording is that subjects describe their recollection of the practice, while the researcher monitors the recording in parallel.

2.2. EQUIPMENT AND ANALYSIS

Recordings were made using 24-bit Mitsar DC amplifiers, either the 31-channel Mitsar 202, or the 21-channel wireless SmartBCI amplifier (Mitsar Medical, St Petersberg). The former having a sampling rate of 500/sec and upper frequency limit of 150 Hz, used with Easycaps and sintered Ag/AgCl electrodes; the latter a sampling rate of 250/sec and upper frequency limit 70 Hz, used with MCScaps and sintered Ag/AgCl electrodes. In using DC amplifiers, choosing the best cap/gel combination is critical to minimise drift and maintain stable low impedances at the electrode-skin interface. Having tested many combinations, we agree with Tallgren *et al*. (2005) that saline-based gels used with sintered Ag/AgCl electrodes are essential with DC amplifiers, and after testing most commercial gels, we favour a combined conductive and mildly abrasive gel to obtain impedances close to or less than 5KΩ, with caps that allow good visual access to the electrode-skin interface to apply gel.

Electrodes were placed according to the international 10-20 system, with a monopolar linked-ears reference. Software analysis was carried out using WinEEG, implementing the Infomax algorithm as used in EEGLAB (Delorme and Makeig, 2004) to compute spectra and independent components (ICs). Cortical sources were computed using the reverse solution of eLoreta (Pascual-Marqui, 2007). Bandwidth and epoch length are important variables in computing spectra and ICs for the different features we observe; that is, spindles, slow waves (SWs) and spike-waves (S-Ws). Since the SWs we analyse are very strong against the EEG background, we adopt a broad bandwidth of 0.032-70/150 Hz, depending on the amplifier model, to capture the full range of spectral activity; whereas for spindles a bandwidth of 5.3-15 Hz is used to minimise confusion with SWs and higher frequency beta and gamma activity; and for S-Ws, 0.53-70/150 Hz, again to minimise SW confusion, but to retain high frequency content given the harmonic structure of the S-Ws.

Epoch length introduces a smoothing effect of its own irrespective of the pass-band, such that epochs of 4, 8, 16, 32 and 64 secs smooth frequencies below 0.25, 0.125, 0.063, 0.031 and 0.016 Hz respectively. To capture SW activity, we use epochs of 16 or 32 secs depending on the length of segment analysed; for spindles we use 4 secs; and for the very brief S-W bursts we use the shortest WinEEG epoch of 1 sec; all with 50% overlap Hanning windows.

2.3. ARTEFACTS OR CORTICAL?

With atypical EEG phenomena, the question of what is artefact and what is cortical is an important question, with the risk of discarding important cortical activity if some unusual feature is too quickly labelled “artefact”. Accordingly, the experimental design aims, as far as possible, to prevent artefacts arising in the first place. In an early pilot study, movement and eye artefacts were a concern, the former caused mainly by movement of electrode connector wires if a subject moves during recording. For the 31-electrode system the most effective solution has been to gather the electrode wires into an “umbilical cord” sheathed in earthed carbon-fibre material between headcap and amplifier; whereas the 21-channel system is already resilient to movement artifacts due to short connections to the wireless amplifier mounted directly on the headcap. Combined with subjects experienced in meditation, used to holding

bioRxiv preprint doi: https://doi.org/10.1101/407544; this version posted January 15, 2019. The copyright holder for this preprint (which was not certified by peer review) is the author/funder. All rights reserved. No reuse allowed without permission.

still postures for long periods, as well as the observer/researcher noting posture changes or signs of muscle tension, very few segments have needed to be excluded. The only situation where movement remains a problem is when recording the deliberate arousal of high intensity clonic epileptiform states, where the task of separating movement artefact from cortical activity is a work in progress.

For eye artifacts, visual inspection can recognise most types, and we have chosen not to use automated software-removal algorithms to avoid confusion with atypical frontal delta and SW activity seen in this form of meditation. Visual inspection confirms that the bulk of the frontal activity is quite different to eye-blink artefacts, or lateral eye tracking; for example, if it does occur it is far slower than eye blinks, and is mostly not restricted to frontal EEG sites. However, some cases remain where localised frontal activity may be affected by eye-tracking; these we exclude from detailed SW source analysis, focusing instead on those cases where SWs develop sustained high intensities and clear rhythmicity, across multiple electrode sites. In a few cases, some meditators display eye-flutter due to over-concentration, and since spike-wave activity is sometimes also observed, this flutter may be related to eyelid myoclonia (Joshi and Patrick, 2007) seen in absence epilepsy. If it does occur, flutter usually settles down during a recording, but we have found that soft cotton-wool pads held gently in place on the eyelid by lightweight spectacles effectively damps down the physical effects of such activity.

On any remaining occasions where doubt remains about artefacts, those sections are excluded, and all EEG activity analysed in this paper comes from uninterrupted sections to avoid problems of interpolation. The fact that recognisable themes and patterns of cortical sources are found in recordings carried out over several years, using two different amplifiers, with some subjects re-recorded after intervals of 1-3 years, adds to our confidence that we are dealing with patterns of cortical activity inexplicable by artefacts or flawed methodology.

3. RESULTS

Table 1 is an overview of EEG recordings of 29 subjects during 2014-18, most carried out during 10-day intensive meditation retreats. Two (subjects 4, 22) were excluded due to impedance problems, leaving 27 subjects. Six of these were re-recorded after intervals of 1-3 years, giving 35 independent recordings. As described in section 2.1, our protocol is to examine themes of EEG activity as meditators with widely varied experience attempt to develop jhāna meditation, then examining those themes against Buddhist understandings of the different jhānas. Visual inspection yields three striking features:

1. Spindles: 22 subjects (28 recordings) show significant spindle activity ("Yes", column 3), and 18 recordings are analysed in more detail in Table 2. By spindles we refer to the occurrence of "wave-packets", similar to those found in stage 2 nREM sleep, rather than more continuous EEG activity.
2. Slow waves (SWs): 15 subjects (22 recordings) show varying levels of SW activity ("Yes", column 4). Those which are well-defined, frequent or very-frequent against background EEG, and extensive over the head reducing risk of confusion by frontal eye-artifacts, are of particular interest and share similar features. Within this group, subjects 3, 5, 17, 24 and 26 develop SWs of very high levels of intensity, in long trains of well-defined near-sinusoidal morphology, completely dominating the EEG. Such powerful and clearly defined SW activity is very suited for cortical source reconstruction. Two other subjects, 14 and 19, also show very strong and well-defined SWs, but of a quite different nature; isolated, with long silences between, and affecting only frontal and temporal sites; we suspect a different underlying mechanism for these, and reserve their analysis to a future paper.
3. Seizure-like phenomena (column 5): for example, discrete bursts of spike-waves (S-Ws) for 8 subjects, and the ability of some subjects to intentionally evoke clonic epileptiform activity.

Subjects	**Rest**	**Meditation**			**Comments**
Year recorded Years' practice (of which jhāna).	**Eyes-closed activity (p-p) µV**	**Spindles Density sp's/min. Extensive vs mainly occipital.**	**Slow-waves (SWs) Very frequent >50%; frequent 20-50%; infrequent <20%. Well-defined or ill-defined. Extensive, isolated or travelling. p-p µV and approx. ½ period (secs) by visual inspection.**	**Spike-wave (S-W) bursts**	

bioRxiv preprint doi: https://doi.org/10.1101/407544; this version posted January 15, 2019. The copyright holder for this preprint (which was not certified by peer review) is the author/funder. All rights reserved. No reuse allowed without permission.

1 2014 41 (6) **2015** 42 (7) **2016** 43 (8)	~40-50 ~20-40 ~20-30	Yes, 20-35/min, extensive. Yes, 15-30/min, extensive but ill-defined. Yes, 25-35/min, extensive.	Yes, frequent, ill-defined, extensive, not clearly travelling; ~130-200 µV p-p; ~5sec Yes, infrequent, ill-defined, extensive, not clearly travelling; ~100-200 µV p-p; ~4-10 secs. Yes, infrequent, ill-defined, mainly frontal, not travelling; ~150-250 µV p-p; ~3-6 secs.	No. Yes, occipital S-Ws ~5.37 Hz, well-defined Yes, occipital S-Ws ~4.88 Hz, ill-defined.	Periods of high gamma superposed on SWs. Ditto. -
2 2016 39 (4)	~20-35	Yes, 15-25/min, mainly occipital.	Yes, infrequent, ill-defined, frontal, not travelling; ~50-150 µV p-p; indeterminate periodicity.	No.	-
3 2014 52 (20) **2015** 53 (21) **2017** 55 (23)	~25-35 ~40-55 ~40-50	Yes, 3-8/min, occipital but ill-defined. Indeterminate. Yes, 3-8/min, extensive but ill-defined.	Yes, infrequent, ill-defined, extensive, not travelling; ~100-125 µV; ~3-6 secs. Yes, very frequent, well-defined, extensive, travelling; ~150-400 µV; ~3-5 secs. Yes, very frequent, well-defined, extensive, frontal-occ. antiphase; 200-400 µV; 3-5 secs.	No Yes, occipital S-Ws ~5.36 Hz, well-defined No.	- Single brief burst of frontal S-Ws ~3.2 Hz. -
4 2014 16 (2)	n.a.	n.a.	n.a.	n.a.	Not used – impedances problem.
5 2014 30 (7) **2017** 33 (10)	~20-35 ~30-45	No. No.	Yes, very frequent, well-defined, extensive, travelling; ~400-900 µV; ~4-6 secs. Yes, very frequent, well-defined, at Cz & CPz, near-simultaneous; ~400-2000 µV; ~4-6 secs.	No. No.	Frontal and occ. gamma modulated by SWs. Strong occipital gamma modulated by SWs.
6 2015 39 (4)	~30-40	Yes, 15-22/min, extensive.	Weak, absent or indeterminate, except some infraslow-wave activity during arousing of *piti*.	Yes, during arousal of *piti*, ~3.91 Hz, well-defined.	
7 2015 28 (5)	~30-50	Yes, 15-25/min, extensive.	Weak, indeterminate, except for 2 brief episodes of extensive but ill-defined, not travelling SWs during arousing *piti*; ~150-200 µV.	Yes, during arousal of *piti*, ~5.85 Hz, well-defined.	
8 2015 37 (4)	~25-35	Yes, 5-15/min, extensive, but ill-defined.	Irregular and atypical SWs with repeated phase-reversals ~150-200 µV; indeterminate period.	No.	Query T6 electrode problem? Atypical SWs; other biological cause?
9 2015 6 (2)	~30-40	Yes, 10-18/min, extensive.	Weak and irregular mainly frontal, 100-150 µV; later develop occipitally, 150-200 µV; ~7-10secs.	No.	
10 2015 32 (5) **2016** 33 (6)	~30-40	Yes, 10-20/min, mainly occipital. Ditto.	Yes, frequent but ill-defined, mainly frontal, non-sinusoidal, not travelling; ~150-300µV; 2-5 secs. Weak, absent or indeterminate.	No. No.	
11 2015, 25 (5)	~30-40	No.	Weak, absent or indeterminate.	Yes, occipital S-Ws ~4.88 Hz, well-defined	
12 2015, 27 (5)	~15-30	Indeterminate.	Weak, ill-defined, frontal, not travelling; 100-150 µV; ~4 secs.	No.	Muscle tension at T3?
13 2016 6 (2)	~30-40	Yes, 8-16/min, extensive but ill-defined.	Weak, ill-defined, frontal, not travelling; 75-150 µV; indeterminate periodicity.	No.	
14 2016 30 (6)	~45-65	Yes, 15-25/min. extensive.	Yes, isolated, well-defined, +ve SWs, initially frontal, travelling to temporal sites, reach >2500 µV p-p; ½ period from peak to minimum ~10 sec	No.	
15 2016 41 (6) **2018** 43 (8)	~30-40	Yes, 8-18/min, extensive. Yes, 10-20/min, extensive, but confused with gamma and S-Ws.	Weak, indeterminate; possible uSWs occasionally at occipital sites. Weak, absent or indeterminate.	Yes, occipital S-Ws ~7.81 Hz, well-defined Yes, occipital S-Ws ~5.35 Hz, well-defined	
16 2016 24 (5)	~30-40	Yes, 12-22/min, mainly occipital..	Yes, frequent but ill-defined & non-sinusoidal, frontal (delta or K-complexes?); ~150-250 µV; ~3-4 secs.	No.	
17 2016 20 (5)	~20-45	No.	Yes, v. frequent, well-defined, extensive, travelling; 800-2500 µV; 3-5 secs.	No.	Frequent ictal spikes at 2.75Hz, mainly occipital.
18 2016 42 (5)	~20-40	Yes, 2-10/min, extensive but ill-defined.	Weak, absent or indeterminate.	No.	
19 2016 33 (6)	~20-40	Yes, 12-20/min, extensive.	Yes, isolated, well-defined, +ve SWs, initially frontal, travelling to temporal sites, reach >2500 µV p-p; ½ period from peak to minimum ~10 sec	No.	
20 2016 7 (2)	~30-40	Yes, 2-8/min, extensive but ill-defined.	Yes, frequent, well-defined but near "square", mainly frontal, not travelling; ~350-500 µV; 4-6 secs.	No.	
21 2016 36 (8)	~25-35	Yes, 9-15/min, extensive.	Weak, infrequent, ill-defined; ~100 µV; 3-5 secs.	No.	
22 2016 42 6)	~25-45	3-6/min, extensive but ill-defined, see Comments.	See Comments	No.	High frontal gamma; or suspect recording - unstable impedances?
23 2016 8 (2)	~30-45	Yes, 4-10/min, extensive but ill-defined.	Yes, infrequent, ill-defined, frontal, not travelling; ~100-200 µV; 4-8 secs.	No.	
24 2016 43 (6) **2017**	~35-55 ~40-60	Yes, 12-20min, extensive. Yes, 5-14/min,	Yes, v. frequent, well-defined, extensive, travelling, 400-600 µV; 3-4 secs. Yes, v. frequent, well-defined, extensive,	Yes, occipital S-Ws ~6.84 Hz, well-defined Yes, occipital S-Ws	- Evidence of spindles

bioRxiv preprint doi: https://doi.org/10.1101/407544; this version posted January 15, 2019. The copyright holder for this preprint (which was not certified by peer review) is the author/funder. All rights reserved. No reuse allowed without permission.

44 (7)		extensive, but see Comment.	travelling, 400-600 µV; 3-5 secs.	~6.84 Hz, riding on SWs.	transforming to S-Ws (to be followed up).
25 2016 4 (1)	~45-55	Yes, 15-25/min, extensive.	Yes, infrequent well-defined, not travelling, mainly frontal; ~100-150 µV; ~3-5 secs.	No.	
26 2016 37 (5)	~50-70	Indeterminate.	Yes, frequent, well-defined, extensive, travelling; ~300-400 µV; 4-5 secs. Also, some isolated +ve SWs later, up to ~2500 µV; 5-8 secs half-period.	Yes, occipital S-Ws ~3.42 Hz, well-defined.	
27 2016 4 (1)	~30-40	Yes, 10-18/min, extensive.	Weak, absent or indeterminate.	No.	Occipital impedances problem; later part of record discarded.
28 2017 40 (6)	~30-40	Yes, 8-16/min, extensive.	Yes, infrequent, well-defined but non-sinusoidal (fast +ve then slow decline), non-travelling, mainly frontal; 120-175 µV; ~6-12 secs.	No.	
29 2017 30 (5)	~20-35	Yes, 8-18/min, Extensive	Weak, infrequent, ill-defined, mainly frontal; ~80-120 µV; periodicity indeterminate.	No.	

Table 1 Study **p**articipants: 29 subjects, 37 independent recordings 2014-18. "Extensive" = affecting more than half the electrode sites; p-p = peak to peak; "very frequent", "frequent", "infrequent" = percentage of SWs per minute; "well-defined", "ill-defined" = clarity of SWs against EEG background. This overview is based on visual inspection to show emerging themes, prior to detailed analysis.

The presence of persistent and strong SWs, and spindles, invites comparison to nREM sleep, anaesthesia and coma, while the occurrence of S-Ws is reminiscent of absence epilepsy. In this section each theme is taken in turn, with its own discussion, with the findings considered as a whole in the final Summary and Concluding Discussion.

3.1. SPINDLES

Sleep spindles are well-researched in polysomnography (Purcell *et al*., 2017), but spindling is also found in situations of conflicted attention (Sonnleitner *et al*., 2012), as well as during slow induction of propofol and other volatile anaesthetics (Hagihira, 2017). It is therefore important to carefully examine meditation spindles for similarities and differences. Three examples are shown in Figure 1. Some subjects show extensive and widespread spindles (e.g. middle panel), others less extensive, but all those we have recorded show involvement of occipital sites. The upper panel is an example of very well-defined occipital spindles, with a symmetrical waxing/waning morphology similar to that in sleep; the enlarged extract also shows some merging of spindles at right. The middle panel shows widespread spindling across most electrode sites, illustrating how in some cases spindles develop into spike-waves (S-Ws) (Leresche *et al*., 2012), in this case at occipital sites, during which spindling appears suppressed; in this example S-Ws in the 3-sec yellow-highlighted segment have a frequency of 5.37 Hz. The bottom panel again shows widespread spindling, although not as extensive as the middle panel.

To examine spindling separate from SWs and higher frequency beta and gamma activity, a 5.3-15 Hz bandpass is used, 60-sec segments selected where spindle density (spindles/min) is maximised, and where spindle p-p intensities are at least 3x the inter-spindle background intensity. An IC analysis is applied to each segment, and sources computed using eLoreta for the strongest ICs that account for at least 50% of the signals' variance of each sample, with total variance normalised to 50%. Figure 2 is an example for subject 14, 2016, and Table 2 summarizes results for 18 independent records.

The second column in Table 2 lists spindle characteristics based on visual inspection (VI) in accordance with the American Academy of Sleep Medicine scoring guidelines (AASM, 2017), as well as from independent component (IC) spectral analysis. Visual scoring of 30 consecutive spindles at the most spindle-active electrode site for each subject yielded measures of spindle density (spindles/min) and spindle or packet duration in secs, while mean spindle frequency was calculated using the fast Fourier transform feature of WinEEG for each of the 30 individual spindles (the VI frequency, bold, in Table 2) for the full signal variance. In addition, each 60-sec record was decomposing into ICs using eLoreta, to find the frequency peak of the dominant cortical components (the IC value, bold, in Table 2). Since we are primarily interested in underlying cortical sources, the IC spindle frequencies are regarded as more representative, and the distribution of those values compared to sleep slow waves is shown at the bottom of Table 2, in comparison to the frequency bands of sleep spindles.

bioRxiv preprint doi: https://doi.org/10.1101/407544; this version posted January 15, 2019. The copyright holder for this preprint (which was not certified by peer review) is the author/funder. All rights reserved. No reuse allowed without permission.

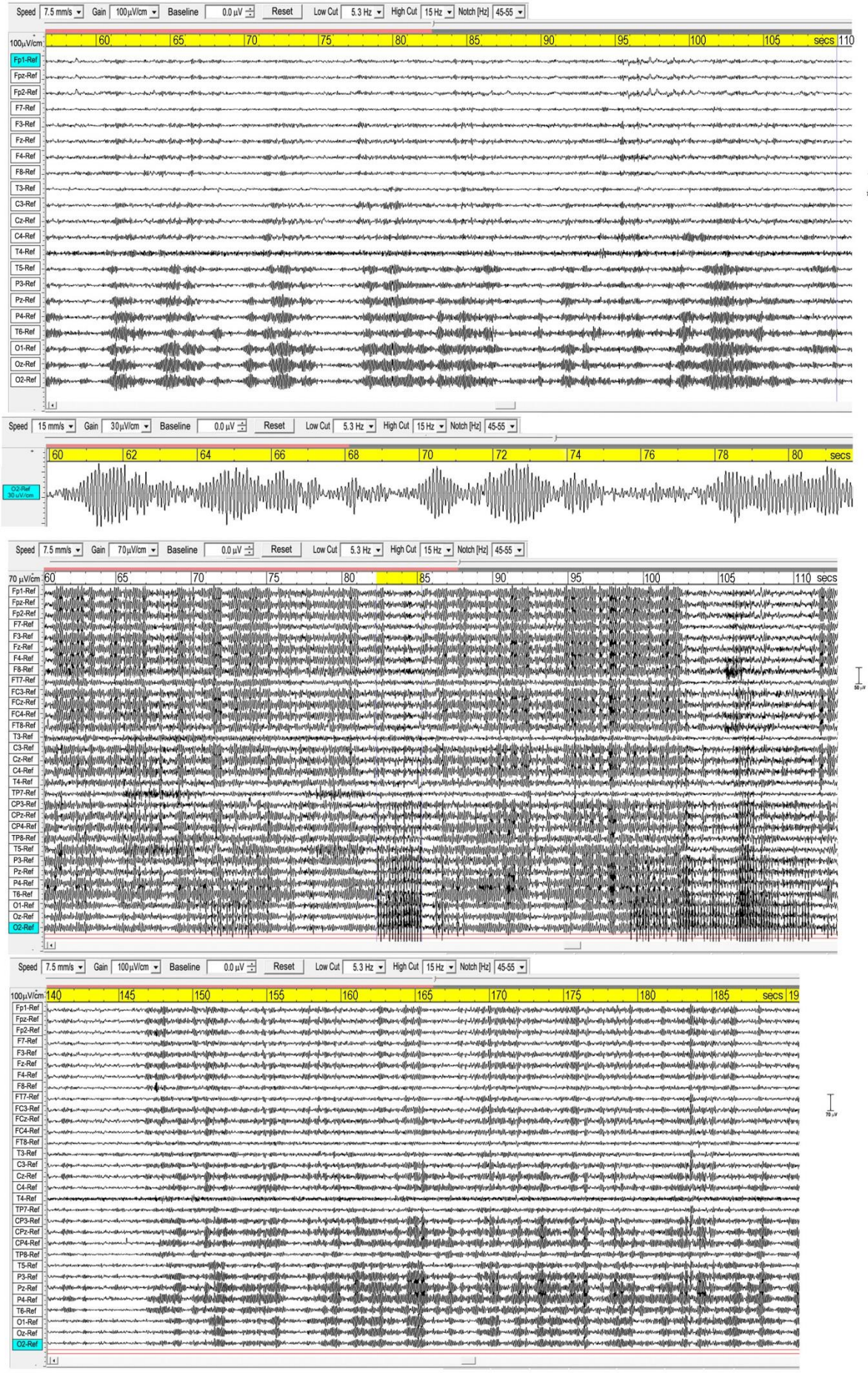

Figure 1 Three examples of spindling. The upper panel is from a recording of subject 16, 2016; the middle panel subject 1, 2015; and the lower panel subject 7, 2015. Bandpass 5.3-15 Hz.

bioRxiv preprint doi: https://doi.org/10.1101/407544; this version posted January 15, 2019. The copyright holder for this preprint (which was not certified by peer review) is the author/funder. All rights reserved. No reuse allowed without permission.

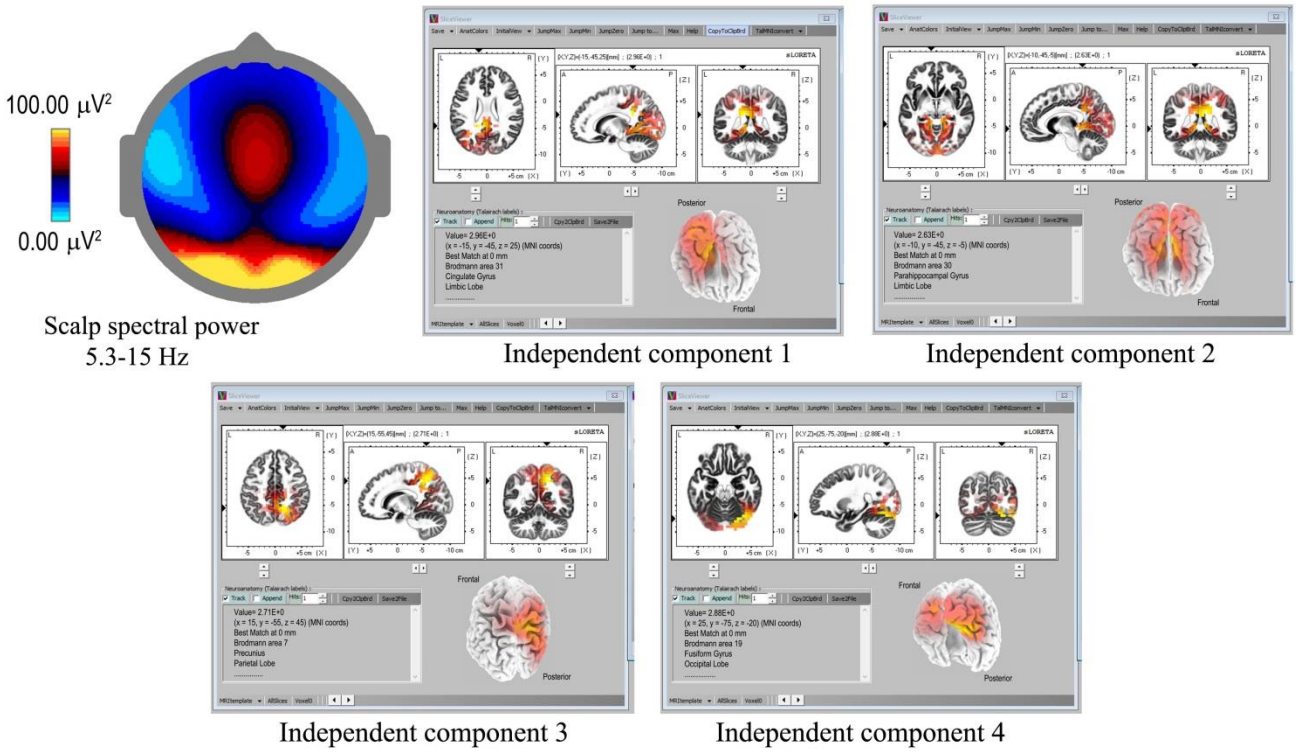

Figure 2 Spindle sources computed using eLoreta for a 60-sec sample of spindles (subject 14, 2016), bandwidth 5.3-15 Hz, 4-second epochs. The scalp mean spectral power distribution at upper left shows maximum intensity in occipital regions, with some extension along the midline. The two strongest sources (ICs 1, 2) are limbic, at Brodmann sites B31 and B30, the cingulate and parahippocampal gyri respectively; and for IC3 and IC4 at B7 (temporal) precunius, and B19 (occipital) the fusiform gyrus.

Columns 3-9 list the cortical sources with MNI (Montreal Neurological Institute) xyz coordinates for the strongest ICs for the 18 records. Subjects 9, 16 and 24 show dominant spindle frequencies of 10.01, 10.25 and 10.50 Hz, respectively, close to those subjects' natural peak alpha frequencies in their (non-meditating eyes-closed) resting state. The remaining subjects show spindle frequencies significantly lower, for subjects 1, 6 and 25 well into the theta band. Other subjects cover the high-theta/low-alpha bands, and subjects 2, 7, 25, 29 show double peaks below the alpha or alpha/theta bands; and in a number of cases we find weaker lower frequency sub-peaks in the IC spectra.

At the bottom of Table 2, sources are summarised into dominant regions of interest (ROIs), normalised to 100% total signals' variance. The anterior-most frontal sources are in Brodmann areas B10, B11, B47, amounting to 8.8%; frontal sources closer to the vertex at Brodmann areas B6, B4, B3, B5 amount to 8.3%; parietal sources at Brodmann B7, B40, B19, 23.5%; limbic sources at Brodmann B30, B31, 10.6%; temporal sources, 25.6%; and occipital sources, 23.2%.

3.1.1 Discussion

First, a comparison to other modalities.

Sleep. Purcell *et al.* (2017) in a major meta-survey of polysomnographic data list the following mean characteristics: spindle density ~0.4-3.5/min; duration ~0.5-1.25 secs; amplitude ~10-50 μV; frequency ~12-14.5 Hz. Strikingly, meditation spindles are much more prolific, with a mean spindle density across the 18 recordings in Table 2 of 13-22/min. This benefits our analysis, since the much higher density against the EEG background greatly reduces problems of confusion with background activity. This is confirmed by spindle frequencies from VI being not greatly dissimilar to those from the ICs, as listed in Table 2. The mean spindle duration from Table 2 is 1.46 ± 0.06 secs, significantly higher than that for sleep spindles, whilst the amplitudes of meditation spindles are similar to those in sleep, ~10-50 μV.

Subject **Year** **Sample-length**	**Spindle Dynamics:** **Density sp./min** **Packet duration (secs)** **Frequency (Hz)** **VI=visual inspection** **IC= indept. components**	**B10** **SFG** **(Frontal lobe)**	**B11/B47** **MFG SFG** **IFG Rectal** **(Frontal lobe)**	**B6/B4/B3/B5** **SFG PCL** **PCG PCoG** **(Frontal lobe)**	**B7/B40/B19** **pCun SMG IPL** **Subgyral** **(Parietal lobe)**	**B30/B31** **pCing Cing** **PHG** **(Limbic lobe)**	**B20/21/22/37/39/40/42** **ITG MTG STG** **SMG Ang Fus** **(Temporal lobe)**	**B17/B18/B19** **IOccG MOccG Cun** **pCun** **Fus Ling** **(Occipital lobe)**
1. **2014** 60 secs	**(VI)** 20-35/min; 1.54 ± 0.09 secs (N=30); 7.77 ± 0.03 Hz (N=30) **(IC) 7.57Hz** + weak 9.03 Hz	**19.1%** B10 SFG ±5 65 -5					**8.6%** B40 SMG 60 -55 20 **8.5%** B39 MTG -45 -80 20	**7.3%** B18 Ling 5 -90 -20 **6.5%** B19 Fus 40 -65 -20
1. **2016** 60 secs	**(VI)** 25-35/min; 1.59 ± 0.08 secs (N=30); 7.86 ± 0.03 Hz (N=30) **(IC) 7.81Hz** + weak 9.28 Hz				**13.9%** B40 SMG 55 -50 30		**10.2%** B20 Fus 55 -40 -25	**11.1%** B18 Cun -15 -100 15 **8.6%** B19 Fus 35 -70 -20 **6.2%** B19 MOG 30 -95 10
2. **2016** 60 secs	**(VI)** 15-25/min; 1.37 ± 0.07 secs (N=30); 9.04 ± 0.10 Hz (N=30) **(IC) 9.03/9.28 Hz double peak**			**16.5%** B4 PCG -10 -40 60	**9.7%** B40 Subgyral -35 -45 35 **7.0%** B40 IPL -35 -55 40	**10.4%** B30 pCing 20 -55 5		**6.4%** B31 Pcun -5 -70 20
6. **2015** 60 secs	**(VI)** 15-22/min; 1.53 ± 0.08 secs (N=30); 8.33 ± 0.05 Hz (N=30) **(IC) 8.06Hz**		**10.9%** B11 Rectal 5 50 -25 **8.5%** B11 SFG 5 65 -10	**8.9%** B5 PCL 0 -35 60 **9.4%** B3 PCG -20 -40 70	**12.3%** B40 SMG -60 -55 25			
7. **2015** 60 secs	**(VI)**15-25/min; 1.73 ± 0.07 secs (N=30); 9.44 ± 0.04 Hz (N=30) **(IC) 9.77/10.01 Hz (double peak)** + weak 8.06				**15.2%** B7 Pcun 10 -50 55 **11.9%** B7 Pcun -5 -70 35 **10.2%** B7 Pcun -10 -65 40 (ext to PCG)		**6.4%** B22 MTG 65 -50 -10 **6.3%** B39 STG 55 -60 30	
9. **2015** 60 secs	**(VI)** 10-18/min; 1.63 ± 0.07 secs (N=30); 10.15 ± 0.05 Hz (N=30) **(IC) 10.10 Hz** + weak 6.95/8.30/8.54 Hz sub-peaks		**8.4%** B11 MFG ±5 65 -15					**11.0%** B17 Cun ±5 -100 -5 **9.7%** B18 Ling 10 -100 -10 **5.9%** B17 Ling 15 -95 -5 **8.0%** B18 MOG 15 -90 15 **7.0%** B18 Cun 5 -100 15
10. **2015** 60 secs	**(VI)** 10-20/min; 1.34 ± 0.07 secs (N=30); 9.42 ±0.07 Hz (N=30) **(IC) 9.52Hz**			**9.0%** B6 SFG 5 5 70 **3.5%** B6 SFG -5 -5 70			**27.6%** B37 Fus 45 -55 -20 **9.9%** B40 SMG 55 -50 20	
10. **2016** 60 secs	**(VI)** 10-20/min; 1.51 ± 0.06secs (N=30); 9.30 ± 0.10 Hz (N=30) **(IC) 9.28Hz**			**10.5%** B6 SFG 5 15 60		**12.3%** B31 pCing 20 -65 15	**9.0%** B21 MTG 65 -55 0	**18.2%** B19 Cun -20 -95 25
14. **2016** 60 secs	**(VI)** 15-25/min; 1.52 ±0.08 secs (N=30); 9.57 ± 0.05 Hz (N=30) **(IC) 9.52Hz** + weak 9.28 Hz				**10.8%** B7 Pcun 15 -55 45	**17.9%** B31 Cing -15 -45 25 **15.6%** B30 PHG -10 -45 -5		**5.7%** B19 Fus 25 -75 -20
15. **2016** 60 secs	**(VI)** 8-18/min; 1.57 ± 0.08 secs (N=30); 8.94 ± 0.11 Hz (N=30) **(IC) 8.54 Hz** + weak 7.32 Hz			**8.9%** B5 PCL 10 -45 60 **8.1%** B6 PCoG -60 -10 40	**12.1%** B7 Pcun 20 -75 40 **3.4%** B40 IPL 40 -45 40		**4.2%** B42 STG -65 -30 15	**13.3%** B18 IOG -40 -90 -10
16.	**(VI)** 12-22/min; 2.02 ± 0.14 secs					**8.4%** B30 pCing		**17.0%** B19 Fus

2016 60 secs	(N=30); 10.23 ± 0.06 Hz (N=30) **(IC) 10.25Hz**					-10 -55 5		-25 -55 -15 **13.8%** B19 Cun 25 -85 30 **10.8%** B19 MOG 40 -70 5
19. **2016** 80 secs	**(VI)** 12-20/min; 1.39 ± 0.06 secs (N=30); 9.21 ±0.06 Hz (N=30) **(IC) 9.03Hz**				**11.9%** B40 IPL 65 -35 30 **10.8%** B40 IPL 50 -60 40 **8.4%** B19 Pcun 5 -85 40		**11.0%** B20 ITG 65 -10 -25 **7.9%** B39 MTG/Ang -40 -75 35	
21. **2016** 60 secs	**(VI)** 9-15/min; 1.15 ± 0.06 secs (N=30); 9.18 ± 0.07 Hz (N=30) **(IC) 9.28Hz** + weak 7.81 Hz					**10.4%** B31 Cing 20 -25 40	**11.7%** B22 STG 50 -35 0 **9.0%** B19 MTG 50 -80 10	**12.3%** B19 Cun -15 -95 25 **6.6%** B18 Ling -10 -90 -20
24. **2016** 60 secs	**(VI)**12-20/min; 1.68 ± 0.08 secs (N=30); 10.52 ±0.06 Hz (N=30) **(IC) 10.5Hz**		**5.5%** B11 Rectal 5 15 -25 **5.4%** B11 SFG 15 65 -15		**14.9%** B7 Pcun -20 -75 40 **13.0%** B7 Pcun -5 -65 40		**11.2%** B39 STG 55 -60 25	
25. **2016** 60 secs	**(VI)** 15-25/min; 1.10 ± 0.05 secs (N=30); 9.28 ± 0.08 Hz (N=30) **(IC) 8.06 and 9.77 Hz** peaks				**17.6%** B19 Pcun -5 -85 40 **5.4%** B19 Pcun -35 -80 40 **8.6%** B40 IPL 50 -50 25		**9.6%** B39 MTG -35 -65 25	**8.8%** B19 MOG 35 -90 15
27. **2016** 60 secs	**(VI)** 10-18/min; 1.15 ± 0.05 secs (N=30); 9.04 ±0.10 Hz (N=30) **(IC) 9.03Hz** + weak 8.06/10.5 Hz				**6.9%** B40 IPL -60 -40 25	**20.6%** B31 Cing -10 -45 30	**8.6%** B21 MTG -65 -25 -15 **13.9%** B39 MTG/Ang 50 -75 25	
28. **2017** 60 secs	**(VI)** 8-16/min; 1.22 ±0.06 secs (N=30); 8.82 ± 0.20 Hz (N=30) **(IC) 8.30Hz** + weak 7.57 Hz		**10.6%** B47 IFG -50 30 -10 **5.7%** B11 MFG 30 35 -20				**17.1%** B20 ITG -65 20 -20 **16.6%** B20 ITG/Uncus -30 -5 -40	
29. **2017** 60 secs	**(VI)** 8-18/min; 1.16 ±0.06 secs (N=30); 9.44 ± 0.08 Hz (N=30) **(IC) 8.54 and 10.01 Hz**		**5.0%** B47 IFG ±45 35 -5		**7.3%** B40 IPL -65 -35 35		**6.4%** B21 MTG 70 -25 -10 **7.3%** B21 MTG 60 5 -15 **9.3%** B39 STG 55 -60 30	**14.7%** B18 Cun 15 -85 25
Sub-Totals		**19.1%**	**60.0%**	**74.8%**	**211.3%**	**95.5%**	**230.5%**	**208.9%**
Norm. to 100%		**2.1%**	**6.7%**	**8.3%**	**23.5%**	**10.6%**	**25.6%**	**23.2%**
ROIs **Norm. to 100%**		**B10 B11 B47** **Frontal 8.8%**		**B6/B4/B3/B5** **Frontal 8.3%**	**B7/B40/B19** **Parietal 23.5%**	**B30/B31** **Limbic 10.6%**	**Temporal** **25.6%**	**Occipital** **23.2%**

				…….. SLOW SLEEP SPINDLES ……..		**……. FAST SLEEP SPINDLES …….**		
	…….MEDITATION SPINDLES ……..							
Spindle frequency Hz	**7.0**	**8.0**	**9.0**	**10.0**	**11.0**	**12.0**	**13.0**	**14.0**
Occurrence	•	• ●●	• ●●	●●●	●●● ●●	●● ●●●	•	•

bioRxiv preprint doi: https://doi.org/10.1101/407544; this version posted January 15, 2019. The copyright holder for this preprint (which was not certified by peer review) is the author/funder. All rights reserved. No reuse allowed without permission.

Table 2 Spindle sources for 18 independent records, 2014-17, with MNI coordinates. SFG, MFG, IFG = superior, middle, inferior frontal gyri; PCL, PCG, PCoG, Rectal = paracentral lobule, postcentral, precognitive, rectal gyri; Pcun, SMG, IPL = precunius, supramarginal gyrus, inferior parietal lobule; pCing, Cing, PHG = postcingulate, cingulate, parahippocampal gyri; ITG, MTG, STG, SMG, Ang, Fus = inferior, middle, superior temporal, supramarginal, angular, fusiform gyri; IOG, MOG, Cun, pCun, Fus, Ling = inferior, middle occipital gyri, cuneus, precuneus, fusiform and lingual gyri.

While Purcell *et al*. list sleep spindle frequencies in the range 12-14.5 Hz, two distinct types are recognised in the literature (e.g. Werth *et al*., 1997), centred on ~11.5 Hz or ~13.0 Hz. Similarly, Del Felice *et al*. (2014) researching cortical sources, found predominantly frontal sources for slow spindles in the 10-12 Hz band, and parieto-temporal sources with smaller frontal and occipital contributions for 12-14 Hz fast spindles. In our results, both source distributions and spindle frequencies are significantly different to the patterns seen in sleep, as shown in Table 2; slower, extending from the low alpha range down to the theta band, and we do not observe two discrete frequency bands as in sleep, for any subject.

Anaesthesia. It is well-recognised that frontal alpha activity increases during general anaesthesia, while occipital alpha decreases (Hagihira, 2017; Hight, 2017; Gent, 2017). During slow induction of propofol anaesthesia (Hagihira, 2017), such frontal alpha develops into prolific spindle activity, which reduces at deeper levels of anaesthesia. More rapid anaesthesia enhances frontal alpha, but does not develop spindles (Hight, 2017). In all situations a lowering of the alpha frequency is observed, and there is some evidence of longer spindle duration. The spindles during slow induction appear similar to those we find in meditation, except that in all our cases occipital sites are involved, with varying degrees of extension over the scalp, but with frontal sites only weakly affected.

Conflicted attention. In studies of driver-distraction and conflicted attention, Sonnleitner *et al*. (2012) demonstrate enhanced alpha spindling (higher density) even when drivers are not drowsy. Whilst they find the greatest effect over central areas using a common-average EEG reference, when aggregated to other references (mastoid or Cz), they conclude a broad distribution of effects over the cortex, unlike in meditation. Since their study is relevant to driving, i.e. with eyes open, and subject to both visual and auditory distraction, it is not directly comparable to the eyes-closed meditation condition.

Overall, we conclude that meditation spindles differ significantly from sleep spindles – in density, location and frequency – and from the mostly frontal spindles in anaesthesia. On the other hand, anaesthesia and driver distraction both show increases in spindle density, and frequencies lower than the typical alpha range, similar to meditation spindles. All these modalities share in common disruption to attention, either by driver distraction, chemically-induced in anaesthesia, or in the approach to sleep. In accordance with our methodology of relating EEG activity to Buddhist understandings of jhāna (section 2.1), in particular that early stages of developing jhāna require withdrawal of attention from the default sensory consciousness (DCs), we conclude that these meditation spindles represent disruption to the cortical networks that sustain attention in the DCs, but in a manner significantly different to disruption in sleep or anaesthesia, which involve loss of consciousness. Also, the fact that spindling is the most common theme among our 29 subjects, suggests, as we might expect, that those who display spindling are negotiating the early stages of developing jhāna; that is, the stages of access concentration and the first rūpa jhāna, and represent growing success in resisting habitual attention processes of naming (inevitably related to language), recognition and discrimination (heavily visually-determined).

Foxe and Snyder (2011) review other evidence that alpha band activity may act as a sensory suppression mechanism in selective attention, and Jensen and Mazaheri (2010) propose that alpha activity performs an important gating mechanism in interregional communication between brain networks. Furthermore, Grandy *et al*. (2013) show that a person's individual alpha frequency (IAF), predominantly in the range 8-12 Hz across individuals, is remarkably stable across periods of months, in response to a wide range of cognitive tasks. We therefore suggest that alpha activity, disrupted in all these modalities, is an integral

bioRxiv preprint doi: https://doi.org/10.1101/407544; this version posted January 15, 2019. The copyright holder for this preprint (which was not certified by peer review) is the author/funder. All rights reserved. No reuse allowed without permission.

part of the human DCs, certainly more important than older views of alpha as simply an "idling rhythm"; one might even suggest it is the *signature* of the DCs. We are also struck by the fact that the ~100ms periodicity of the alpha rhythm is close to the human reaction time, with implied connectivity to sensorimotor networks and readiness for action.

Since it is generally acknowledged that spindles represent thalamo-cortical interactions (Souza *et al*., 2016), we conclude that in this form of meditation changes occur in related thalamo-cortical networks as a result of meditators intentionally withdrawing attention from the default consciousness. How then do the underlying cortical networks compare? We might expect to find involvement of networks related to the dorsal and ventral processing streams heavily involved in attention and visual and auditory processing, that form the "what" and "where" of our DCs experience (Cloutman, 2012; Milner, 2017); as well as changes to networks supporting memory and spatial and temporal orientation, integral parts of our DCs experience of self. Table 3 summarizes the ROIs from the detailed findings of Table 2, and, given the limitations to spatial resolution of 31 or 21 electrodes, the overall picture fits surprisingly well with our hypothesis. Although there is some overlap with cortical sources found for sleep spindles, as in Del Felice *et al*. (2014), the pattern is notably different. The significant presence of limbic sources supports our expectation of effects on memory and spatial and temporal orientation, in accord with Kravitz *et al*'s (2011) view of limbic involvement in the ventral pathway. The ventral pathway links occipital sources via temporal and limbic sources, to frontal sources; while the dorsal pathway links to frontal sources via fronto-parietal networks. This is an average picture across 15 subjects, and no individual subject shows a clear preference for one or other path.

<table>
<tr><td>SPINDLES SUMMARY
16 subjects
(18 records 2014-17)
Bandpass 5.3-15 Hz
4 sec. epochs</td><td>B10
SFG

Frontal Lobe
z-coord -5</td><td>B11 B47
MFG SFG
IFG Rectal

Frontal Lobe
z-coord -10–-25</td><td>B6 B4 B3 B5
SFG PCG PCL PCoG

Frontal Lobe
z-coord +40–+70</td><td>B7 B40 B19
Pcun SMG IPL Subgyral

Parietal Lobe
z-coord +25–+55</td><td>B30 B31
Cing pCing PHG

Limbic Lobe</td><td>B20/B21/B22/B37/
B39/B40/B42
ITG MTG STG
SMG Ang Fus

Temporal Lobe</td><td>B17/B18/B19
IOccG / MOccG
Cun pCun
Fus Ling

Occipital Lobe</td></tr>
<tr><td>Sub-Totals</td><td>19.1%</td><td>60.0%</td><td>74.8%</td><td>211.3%</td><td>95.5%</td><td>230.5%</td><td>208.9%</td></tr>
<tr><td>Norm. to 100%</td><td>2.1%</td><td>6.7%</td><td>8.3%</td><td>23.5%</td><td>10.6%</td><td>25.6%</td><td>23.2%</td></tr>
<tr><td rowspan="2">ROIs
Norm. to 100%</td><td colspan="2" rowspan="2">B10 B11 B47
Frontal
8.8%</td><td>B6/B4/B3/B5
Frontal
8.3%</td><td>B7/B40/B19
Parietal
23.5%</td><td>Limbic
10.6%</td><td>Temporal
25.6%</td><td rowspan="2">Occipital
23.2%</td></tr>
<tr><td colspan="2">Dorsal pathway</td><td colspan="2">Ventral pathway</td></tr>
</table>

Table 3 Meditation **s**pindle sources, ROIs, from Table 2, with the same abbreviations.

3.2. SLOW-WAVE (SW) ACTIVITY

We consider SWs as falling within the frequency band 0.1-1.0 Hz, to distinguish from delta activity in the 1.0-4.0 Hz band. Figures 3 and 4 show six independent recordings illustrating some main features. The EEG electrode sites are labelled at the left, from frontal (F) sites at the top, to occipital (O) sites at the bottom (with T, C, P denoting temporal, central and parietal areas). The top bar shows time in secs. Figure 3, top panel (subject 5, 2014), shows intense SWs at frontal, occipital and central-temporal sites. The inset scalp intensity distributions correspond to the start and end points of the yellow-highlighted interval in the time bar, showing a pattern of alternating SW inhibition-excitation, which in this example reaches 1350 μV peak to peak (p-p) at CPz. The middle panel is the same subject recorded again in 2017, now with more experience of jhāna meditation, showing highly focused activity near the vertex at Cz and CPz (highlighted by the inset scalp maps) with p-p values >1500 μV, and much reduced frontal and occipital activity. The form of the SWs is also different, with a more rapid +ve onset, and slower recovery, reminiscent of patterns found for relaxation oscillators

bioRxiv preprint doi: https://doi.org/10.1101/407544; this version posted January 15, 2019. The copyright holder for this preprint (which was not certified by peer review) is the author/funder. All rights reserved. No reuse allowed without permission.

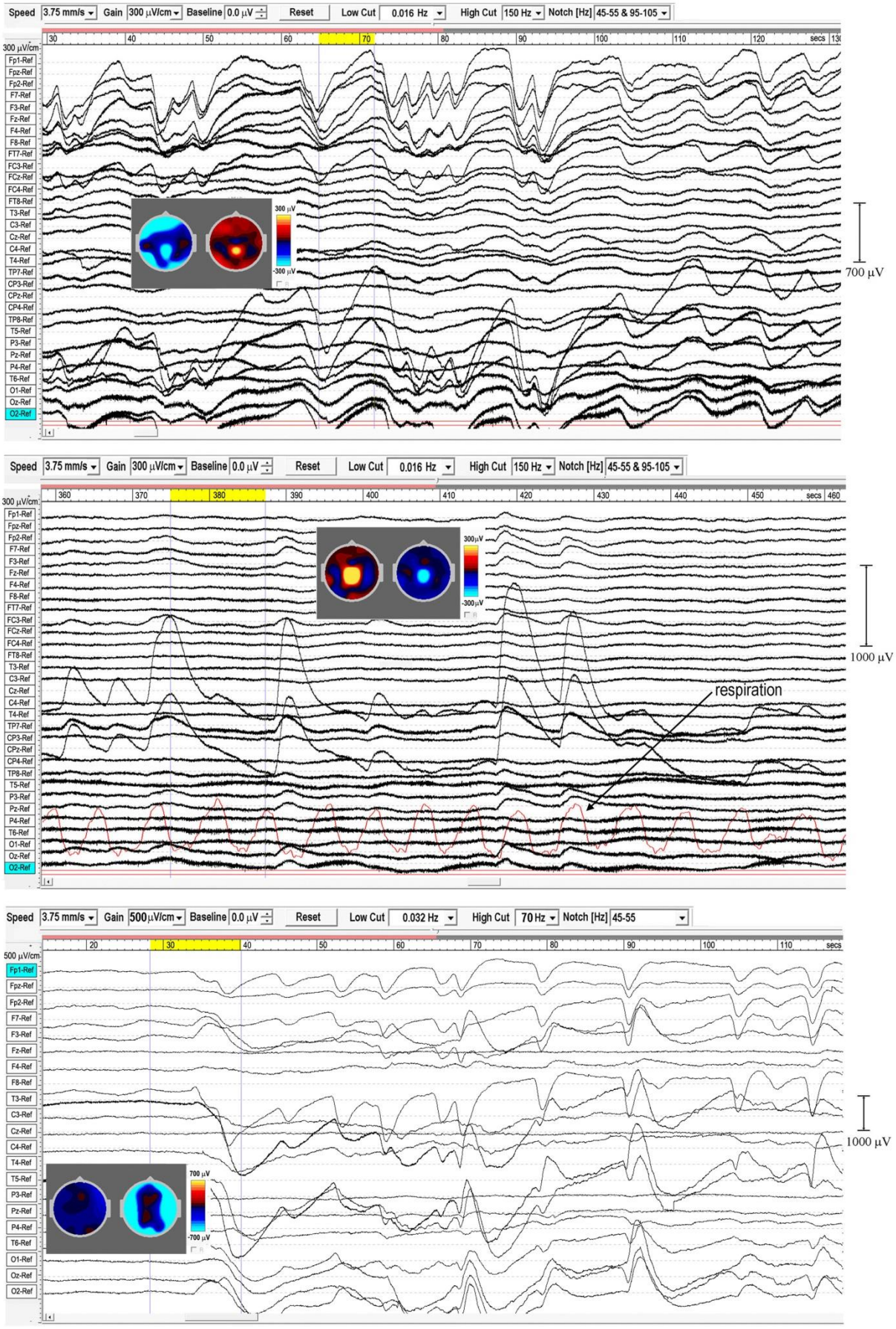

Figure 3 Extensive and powerful slow waves during Samatha meditation. Top panel subject 5, 2014; middle panel subject 5, 2017; bottom panel subject 17, 2016. The inset scalp intensity maps correspond to the start and end points of the yellow-highlighted intervals.

bioRxiv preprint doi: https://doi.org/10.1101/407544; this version posted January 15, 2019. The copyright holder for this preprint (which was not certified by peer review) is the author/funder. All rights reserved. No reuse allowed without permission.

The rate of rise for the SW at 418 secs reaches ~1400 μV/sec. The red trace is respiration, measured by an induction-loop chest belt. The bottom panel, subject 17, 2016, illustrates how SW onset for some meditators can be very rapid; in this case widespread SW activity starts at ~35 secs into meditation, with an initial massive inhibition at 40 secs, with the inset maps showing a complete annulus of inhibition around central areas. The ensuing SWs reach remarkable intensities > 2000 μV p-p at times.

The top panel in Figure 4 (subject 24, 2016) shows SWs particularly strong at occipital sites, with inset maps for the SW at 212-216 secs again showing an annulus of inhibition-excitation enclosing central areas. This subject also shows brief periods of enhanced gamma activity (e.g. at 206-12 secs), as well as spike-wave (S-W) bursts lasting 2-6 secs at occipital sites. The middle panel shows the same subject in 2017, now with much stronger SW activity at sites around the vertex (as in the inset scalp maps) compared to 2016. Occipital SWs are still present, also significant gamma activity, and again S-W bursts at occipital sites as in 2016. In contrast to the above, the lower panel (subject 19, 2016) is one of two examples noted earlier, which we believe illustrates a different mechanism, to be explored separately, of isolated SWs with longer periods of recovery and relative "silences" between. This subject shows fast responsiveness and SW onset similar to subject 17 in Figure 3, with a massive positive SW appearing just 5 secs after starting meditation, reaching 2400 μV at Fp2, one of the highest levels we have recorded; travelling ~3.6 secs later to temporal sites T3 and T4. For this subject, the intense SWs are accompanied by strong increases in the gamma band. The scalp maps for the segment 10.5-23.3 secs show the familiar alternation of excitation-inhibition, which in this case is focused at frontal and temporal sites, with occipital sites unaffected.

3.2.1. SW Statistics

Table 4 summarises SW statistics from over 600 SWs from 8 independent recordings of 5 subjects, 2014-17, who show consistent SW activity. Sections showing at least 3 successive SWs were examined in turn, and the periods between successive +ve to +ve, or –ve to –ve peaks measured, according to whether +ve or –ve peaks were dominant (Figure 3, middle panel, is an example of +ve-dominant SW peaks). P-p voltages from either a +ve peak to the following minimum, or from a –ve peak to the following maximum were measured, giving a mean p-p SW amplitude of 417±69 μV, with individual amplitudes ranging from ≤100 μV to 2255 μV. Across all the recordings, the mean SW period was 8.36±0.60 secs, corresponding to a mean SW frequency of 0.125±0.010 Hz.

In some recordings, respiration was measured using an induction-loop chest-belt. Subject 5, 2017, for example (middle panel of Figure 3), showed a mean SW period of 9.59 ± 0.66 secs (Table 4), and a mean respiration period for the same segment of 9.88 ± 0.33 secs, confirming what visual inspection of data for several subjects shows to be a close relationship between SW and respiration frequencies. A more detailed correlation analysis has not been possible to date due to software limitations in WinEEG.

3.2.2 Travelling SWs

The final column in Table 3 gives an indication from visual inspection of the EEG, of the travelling nature of the SWs. In some cases they appear to be near-simultaneous for some 10's of seconds across wide areas, while other sections show frontal sites to lead or lag posterior or temporal sites. As far as we can determine, there is no obvious relation to the stage of a subject's meditation. Subject 5, 2014 (top panel, Figure 3), sustained strong and well-defined travelling SWs, 300-700 μV p-p, for over 20 mins, and provides the clearest example of travelling SWs, one of which is shown in Figure 5, where the scalp intensity maps 1-6 trace the development of the −ve SW peak across a 2.25-second interval (highlighted yellow, top bar). Note the localised midline peak, just posterior to the vertex, extending into occipital areas. Also, the considerable, and typical, broadening of the SW as it reaches occipital areas. Scalp map 1 shows the initial +ve phase of the wave, strongest at left-temporal site T5, and midline central-parietal CPz, less intense frontally. The –ve phase then develops frontally, extending left-frontally, before travelling to occipital areas (mainly left), as in maps 2-6.

bioRxiv preprint doi: https://doi.org/10.1101/407544; this version posted January 15, 2019. The copyright holder for this preprint (which was not certified by peer review) is the author/funder. All rights reserved. No reuse allowed without permission.

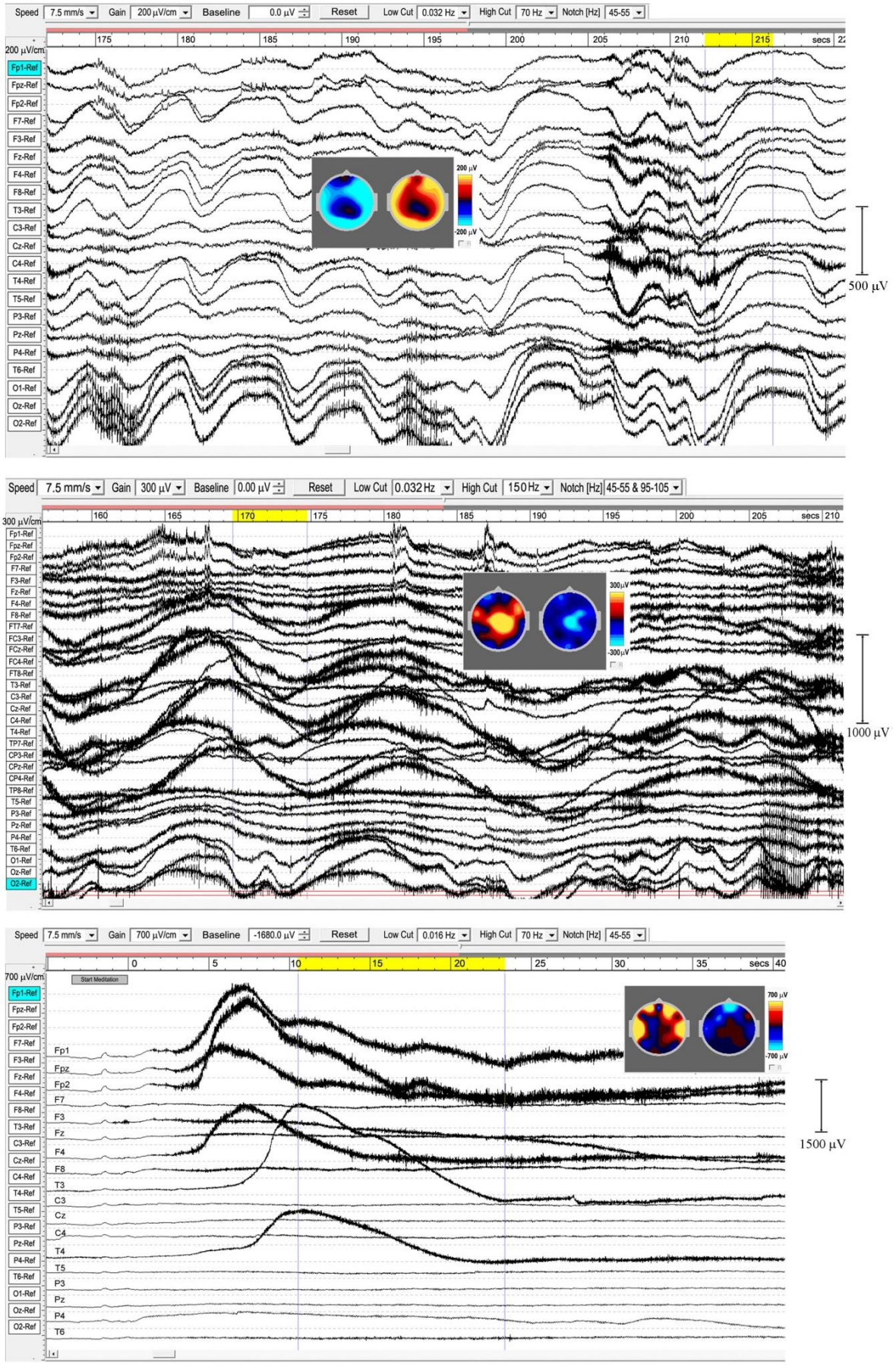

Figure 4 Extensive and powerful slow waves. Top panel subject 24, 2016; middle panel subject 24, 2017; bottom panel subject 19, 2016. Note the posterior spike-wave bursts for subject 24, and the isolated extremely high voltage SW shown by subject 19.

bioRxiv preprint doi: https://doi.org/10.1101/407544; this version posted January 15, 2019. The copyright holder for this preprint (which was not certified by peer review) is the author/funder. All rights reserved. No reuse allowed without permission.

Subject	**Mean period (secs)** between successive positive or negative SW peaks, excluding "silences" (with SE of mean, N = no. of SWs)	**Mean frequency (Hz)** (with SE of mean, N = no. of SWs)	**Mean p-p amplitude (μV)** of successive SWs, from positive peak to following minimum, or negative peak to next maximum, excluding "silences" (with SE of mean, N = no. of SWs)	**Transit time estimates**
5, 2017 At Cz, +ve peaks	9.59 ± 0.66 secs N=91	0.104 ± 0.007 Hz N=91	696 ± 47 μV N=94	Mostly near-simultaneous at Cz and CPz (and to a lesser extent at TP7), ±200 ms.
5, 2014 At CPz, -ve peaks	10.45 ± 0.50 secs N=93	0.096 ± 0.005 Hz N=93	469 ± 26 μV N=99	Frontal to occipital (Fp1 to O1/O2), 593±300 ms. Frontal to temporal (Fp1 to T5), 723±230 ms. Frontal to central (Fp1 to CPz), 1278±340 ms.
3, 2017 At FT7 +ve peaks	8.94 ± 0.47 secs N=108	0.112 ± 0.006 Hz N=108	245 ± 13 μV N=113	Fronto-central +ve peaks in antiphase with central-occipital –ve peaks, ~simultaneous ±200 ms.
3, 2015 At F8, -ve peaks	5.74 ± 0.36 secs N=63	0.174 ± 0.012 Hz N=63	206 ± 14 μV N=67	Frontal sites lead occipital sites by 340±100 ms.
17, 2016 At F8, -ve peaks	6.65 ± 0.31 secs N=85	0.150 ± 0.008 Hz N=85	654 ± 42 μV N=84	Once SWs established, frontal, central and occipital sites near-simultaneous ±300 ms.
24, 2017 At Cz and O1, Near-sinusoidal -ve peaks used	8.07 ± 0.43 secs N=76	0.124 ± 0.007 Hz N=76	492 ± 30 μV N=83	Early in this subject's practice, frontal sites lead central/parietal sites by ~1.5-3.5 secs; later, occipital sites lead frontal sites by ~0.4-0.7 secs.
24, 2016 At O1 and T3, -ve peaks	6.87 ± 0.40 secs N=74	0.146 ± 0.008 Hz N=74	371 ± 21 μV N=71	Mostly simultaneous ±300 ms, but occasionally occipital sites lead frontal sites by ~0.3-0.5 secs.
26, 2016 At Fz and O2, +ve peaks	10.55 ± 0.83 secs N=42	0.095 ± 0.008 Hz N=42	204 ± 27 μV N=38	Frontal sites lead occipital sites by ~0.5-1.0 secs.
Overall means N = total SWs	**8.36 ± 0.60 secs** N=632	**0.125 ± 0.010 Hz** N=632	**417 ± 69 μV** N=649	

Table 4 SW statistics for 5 subjects, 8 independent recordings, 2014-17.

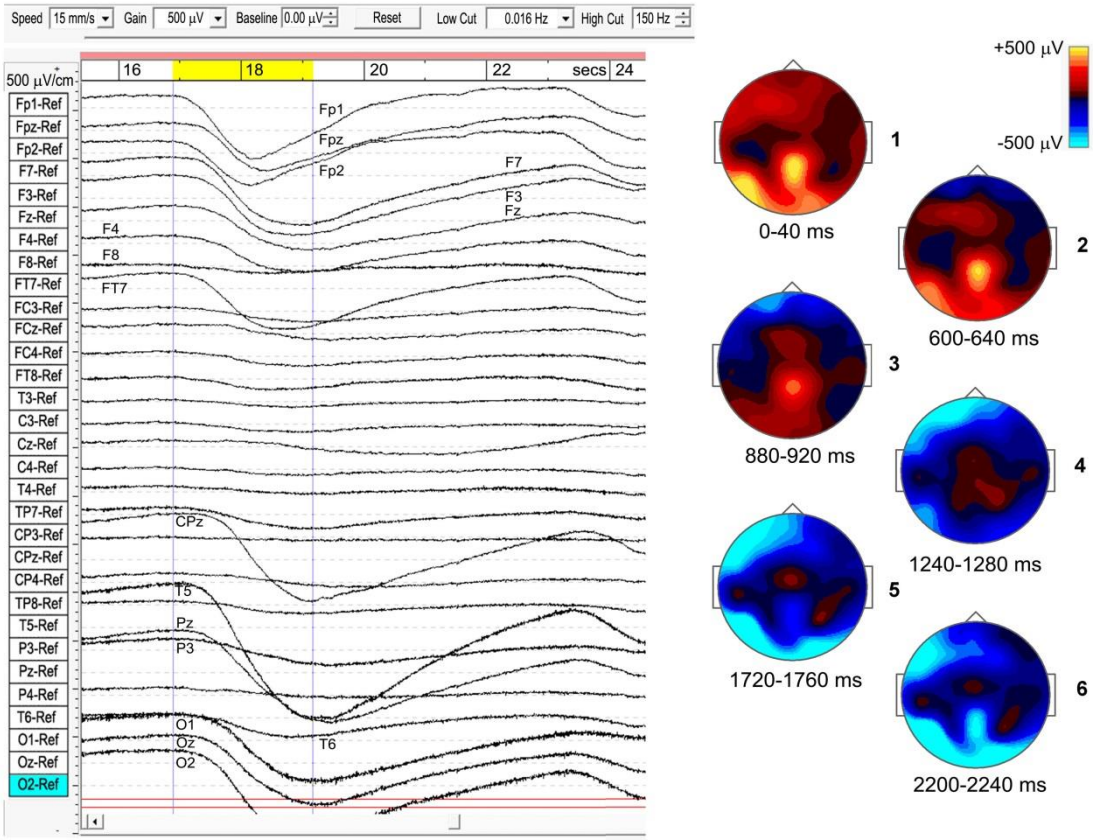

Figure 5 Example of a travelling slow wave (subject 5, 2014), bandpass 0.016-150 Hz.

bioRxiv preprint doi: https://doi.org/10.1101/407544; this version posted January 15, 2019. The copyright holder for this preprint (which was not certified by peer review) is the author/funder. All rights reserved. No reuse allowed without permission.

Maps 1 and 6 in Figure 5 correspond roughly to the excitation-inhibition peaks. The localised midline peak, just posterior to the vertex, is also observed for other subjects who show strongly developed and extensive SWs. Although this is surface EEG activity, the near-vertex peak will be seen to recur in the underlying cortical source analysis.

Although for any particular meditator the sites of activity remain fairly constant during a recording (in this example, EEG sites Fp1, Fpz, Fp2, F7, F3, Fz, F4, FT7, CPz, T5, Pz, O1, Oz and O2), transit times vary considerably as noted for other subjects in Table 4. In this case, the SW in Figure 5 shows a transit time of the –ve peak, front to rear, of ~1200 ms. For 20 successive SWs from this same subject, transit times varied considerably, with means of: frontal (Fp1) to occipital (O1/O2), 593±300 ms; frontal (Fp1) to temporal (T5), 723±230 ms; and frontal (Fp1) to central-midline (CPz), 1278±340 ms. The mean front to rear transit time ~600 ms corresponds to a mean transit speed for this subject of ~50 cm/s across the head, significantly slower than typical values ~1.2-7.0 m/s for sleep SWs (Massimini et al., 2004).

3.2.3. Rhythmic Excitation−Inhibition

The SWs we observe are not random, exhibiting a rhythmic pattern of powerful excitation−inhibition, as shown by the examples in Figures 2 and 3. In some cases the SWs form an almost complete annulus of excitation-inhibition surrounding less affected central areas (e.g. subject 17, 2016, Figure 3; and subject 24, 2016, Figure 4). For other subjects the annulus is only partial, as for subject 5, 2014, Figure 3; and subject 19, 2016, Figure 4. For subjects 5 and 24, re-recorded in 2017 (Figures 3 and 4 respectively) and both with more experience of jhāna, the annulus is replaced by an intense focus near the vertex.

3.2.4. Cortical Sources

Table 5 summarises a source analysis carried out in the same manner as for spindles, for 7 independent recordings (5 subjects) that show the strongest examples of extensive SW activity. Subject 5 was recorded twice, in 2014 and 2017, both with the 31-electrode system; and subject 24 also twice, in 2016 and 2017, with the 21- and 31-electrode systems respectively. To study low frequency structure <1 Hz, epoch length is a key variable as discussed in section 2.2, and depending on the segment lengths in Table 4, epochs of 16 or 32 secs were used. We are therefore confident of capturing frequencies down to 0.03 Hz for five of these recordings (32 sec epoch) and to 0.06 Hz for the other two, particularly given the mean SW frequency of 0.125±0.010 Hz estimated from visual inspection (Table 4).

As with the spindle analysis, cortical sources were computed for the strongest ICs that accounted for at least 50% of the signals' variance for each sample, with the total variance normalised to 50%, using eLoreta. Averaged across all 7 recordings (>2500 secs of strong and persistent SWs), sources are found in: frontal sites, Brodmann B10, B11, B9 (24.1% of the total variance across all recordings); at frontal midline B6 just anterior to the vertex (25.2%); at parietal midline B5, B7 just posterior to the vertex (19.2%); at temporal B20, B21, B22, B37 (11.7%); and at occipital sites B18, B19 (19.8%).

The ROIs are summarised in Figure 6, with 3D source maps to aid visualisation, based on superposition of individual components computed from eLoreta that contribute to each ROI. The midline area near the vertex, bridging the frontal-parietal junction is the dominant ROI, accounting for 44.4% of the total signals' variance. Others are, temporal sources (11.7%), predominantly left and diffuse, merging with, again predominantly left, inferior and middle-occipital sources (10.6%), and finally at far right the midline cuneus (9.2%).

Subject Individual source contributions normalised to 50%	B10 MFG SFG (frontal lobe) X +ve/-ve = R/L	B11 MFG SFG (frontal lobe) X +ve/-ve = R/L	B9 SFG MFG (frontal lobe) X +ve/-ve = R/L	B6 MFG SFG PCL PCoG (frontal lobe) X +ve/-ve = R/L	B5 PCG (parietal lobe)	B7 PCG pCun (parietal lobe)	B20/B21/B22/ B37 MTG ITG STG (temporal lobe) X +ve/-ve = R/L	B18/B19 MOG / IOG Cun (occipital lobe) X +ve/-ve = R/L
3. 2015 0.032-150 Hz 170s segment 16s epochs	**9.0%** B10 MFG 35 60 -5	**5.1%** B11 MFG 10 65 -15				**26.9%** B7 PCG -5 -55 70		**9.0%** B18 MOG 20 -100 0
5. 2017 0.032-150 Hz 360s segment 32s epochs				**27.9%** B6 MFG 5 -15 70 **12.9%** B6 MFG 5 -25 70 **9.2%** B6 MFG -5 -20 70				
5. 2014 0.032-150 Hz 600s segment 32s epochs				**15.7%** B6 PCL 5 -35 70	**20.9%** B5 PCG 5 -45 70	**7.1%** B7 PCG 5 -55 70 **4.2%** B7 PCG -5 -55 70	**2.1%** B37 MTG -60 -50 -10	
17. 2016 0.032-70 Hz 300s segment 32s epochs		**10.8%** B11 SFG -25 55 -15					**16.1%** B22 STG -60 -60 15	**15.1%** B18 Cun ±15 -100 15 **8.0%** B18 Cun ±5 -100 15
24. 2016 0.032-70 Hz 343s segment 32s epochs	**5.5%** B10 MFG 35 60 -10 **4.6%** B10 SFG -35 50 30	**9.7%** B11 SFG 10 65 -10 **6.6%** B11 SFG 15 65 -15	**2.0%** B9 MFG 10 50 40	**5.5%** B6 SFG -20 10 70 **3.0%** B6 SFG -5 5 70 **3.1%** B6 PCoG 25 -15 70				**10.0%** B18 IOG -40 -90 -5
24. 2017 0.032-150 Hz 400s segment 32s epochs		**0.7%** B11 MFG 5 65 -15 **5.2%** B11 MFG -40 55 -10		**6.5%** B6 MFG 5 -25 70 **4.5%** B6 MFG -5 -30 70		**8.0%** B7 PCG 5 -55 70	**7.0%** B21 MTG 65 -55 0	**18.1%** B19 MOG -40 -90 -5 Extends through temp G to ~ -65 -10 -15
26. 2016 0.032-70 Hz 203s segment 16s epochs	**1.5%** B10 MFG -30 55 -10	**12.0%** B11 SFG -20 65 -10	**1.8%** B9 SFG 10 50 35 **9.7%** B9 SFG ±10 55 40				**15.7%** B20 ITG -65 -25 -20	**9.3%** B18 Cun ±5 -100 15
TOTALs **Normalised to 100%**	**20.6%** **5.9%**	**50.1%** **14.3%**	**13.5%** **3.9%**	**88.3%** **25.2%**	**20.9%** **6.0%**	**46.2%** **13.2%**	**40.9%** **11.7%**	**69.5%** **19.8%**
ROIs **Normalised to 100%**	**B10/B11/B9 Frontal** **24.1%**			**B6 Frontal midline vertex** **25.2%**	**B5/B7 Parietal midline vertex** **19.2%**		**B20/B21/B22/B37 Temporal** **11.7%**	**B18/B19 Occipital** **19.8%**

Table 5 Cortical sources for 7 recordings, with epoch lengths 16 or 32 secs according to segment length. MFG, SFG, PCG, MTG, ITG, STG, MOG, IOG, PCoG, PCG = medial frontal, superior frontal, postcentral, middle temporal, inferior temporal, superior temporal, middle occipital, inferior occipital, precognitive and postcentral gyri; PCL = paracentral lobule; pCun = precunius; Cun = cuneus. Each contributing source is listed with its MNI xyz coordinates.

bioRxiv preprint doi: https://doi.org/10.1101/407544; this version posted January 15, 2019. The copyright holder for this preprint (which was not certified by peer review) is the author/funder. All rights reserved. No reuse allowed without permission.

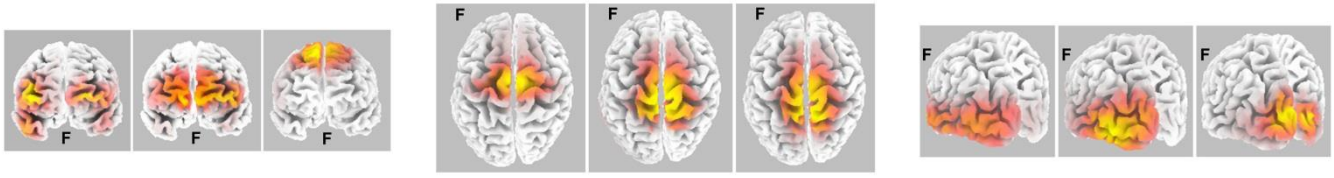

Frontal			Frontal midline vertex	Parietal midline vertex		Temporal	Occipital	
							B18/B19	
B10	B11	B9	B6	B5	B7	B20/21/22/37	IOG/MOG	Cuneus
5.9%	14.3%	3.9%	25.2%	6.0%	13.2%	11.7%	10.6%	9.2%
24.1%			44.4%			11.7%	19.8%	

Figure 6 Summary of SW regions of interest, based on Table 5, for 7 independent recordings of 5 subjects, 2014-17. The 3D cortical source plots are computed using eLoreta, superposing plots for individual components (ICs) that contribute to each ROI.

3.2.5. Infra-Slow-Wave (ISW) Activity

Infra-slow EEG activity (defined here as 0.01-0.1 Hz) has been little studied in the literature, largely due to difficulties with DC drift and confusion with noise and artifacts, as well as the requirement of long records to allow epochs ideally greater than 60 secs. We have two examples of particularly strong SW activity where the raw data suggest an underlying rhythm slower than the mean 0.125 Hz SW frequency of Table 4. However, spectral analysis using WinEEG is not reliable below ~0.02 Hz because of software and epoch limitations already noted, so at this point we rely on visual inspection of the EEG data, with spectral analysis as a tentative comparison.

Figure 7 shows sections from subjects 17 (2016) and 5 (2017) with, to the right, superposed SWs from longer segments (300 and 600 secs respectively) showing a similar morphology of rapid leading edge with much slower over-shooting recovery. The superpositions show half-periods ~21 and ~26 secs respectively, suggesting an underlying ISW frequency of ~0.02 Hz. Bearing in mind the software limitations noted above, a spectral analysis of a 600-sec segment from subject 5, using 64-sec epochs and 0.016 Hz low cut, shows some evidence of a peak at 0.02-0.03, and also at 0.05 Hz.

The lower part of Figure 7 illustrates the overwhelming dominance of SW activity near the vertex for subject 5 in 2014 and 2107. The overall % contributions of ROIs calculated from all 31 ICs for each year from 600-sec samples are shown; being 5.7% frontal, 92.8% vertex and 1.1% occipital in 2014; and 0.2% frontal, 99.7% vertex and 0.1% occipital in 2017. To examine what remains apart from SW activity, the strongest IC spectra were computed using a 5.3-150 Hz bandwidth and are shown at each side, with scalp intensity distributions, revealing broadband gamma activity with only small residual traces of alpha activity, particularly weak in 2017.

3.2.6. Discussion

At first sight the SWs we observe are reminiscent of those in deep (stage 4) nREM sleep, or high-voltage delta coma, or to a lesser extent anaesthesia (where delta activity is notably less rhythmic and coherent). However, meditation SWs (Table 4) are significantly slower and higher voltage (means of 0.125 Hz and 417 μV p-p) compared to those in sleep or coma (0.8-1.2 Hz and 100-300 μV p-p; Libensen, 2012; Sutter and Kaplan, 2012). Indeed, several subjects display intensities reaching over 2000 μV p-p, unprecedented as far as we are aware anywhere in the literature, for any modality. Furthermore, meditation SWs are significantly more rhythmic and extensive than those seen in sleep, and tend to form an annulus of alternating excitation-inhibition around relatively untouched central areas, apart from a localised region near the vertex. It is tempting to take a metaphor from sleep studies and infer that extensive areas of the cortex are "put to sleep", or suppressed, by these high-voltage rhythmic SWs, yet the subjective experience does not support this, since meditators describe an experience of enhanced consciousness, rather than any diminution.

bioRxiv preprint doi: https://doi.org/10.1101/407544; this version posted January 15, 2019. The copyright holder for this preprint (which was not certified by peer review) is the author/funder. All rights reserved. No reuse allowed without permission.

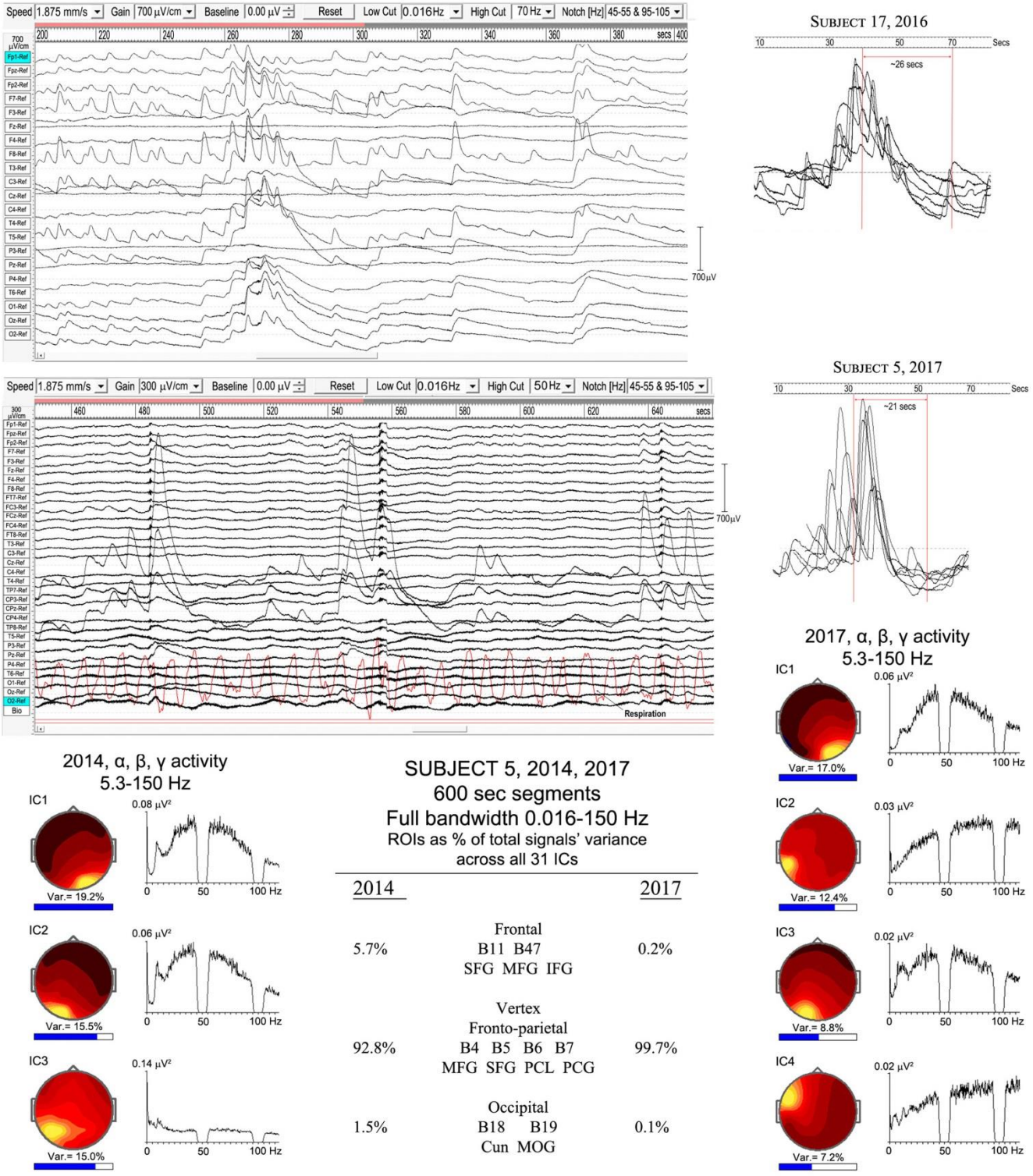

Figure 7 Infraslow-wave (ISW) activity: top panel, subject 17 (2016); middle panel subject 5 (2017). Below is a comparison of the highly focused vertex activity for subject 5 in 2014 and 2017, with the strongest ICs from 600-sec samples for each year shown, and the overall % contributions of ROIs across all 31 ICs for each year. At each side, the IC spectra show higher frequency activity only (bandwidth 5.3-150 Hz), revealing broadband gamma with only small residual traces of alpha activity.

In any case, the surface distribution is quite different to that in sleep, where the scalp power maps show a strong frontal predominance with a smaller occipital focus (Bersagliere *et al*., 2017). Meditation SWs also show a travelling nature as in sleep, but much slower, as in the Figure 5 example of ~50 cm/sec

bioRxiv preprint doi: https://doi.org/10.1101/407544; this version posted January 15, 2019. The copyright holder for this preprint (which was not certified by peer review) is the author/funder. All rights reserved. No reuse allowed without permission.

compared to the range 1.2-7.0 m/sec in Massimini *et al*., (2004) for sleep.

In summary, there are very significant differences to SWs found in other modalities, and this also applies to underlying cortical sources. Our analysis reveals a dominant midline vertex ROI, bridging the frontal-parietal divide, with frontal and occipital regions second and temporal sources third. In sleep, Murphy *et al*. (2009) find the lateral sulci to be a major ROI, together with the medial, middle and inferior frontal gyri, the anterior and posterior cingulate, and the precuneus. More recently, in an eLoreta analysis similar to ours, Bersagliere *et al*. (2017) find a predominantly frontal source distribution. The significance of our observed ROIs in terms of the stages of jhāna, and implications for consciousness will be discussed in the Summary and Concluding Discussion.

The frequency of SWs in sleep or coma is believed to be determined by haemodynamic pressure (Mensen *et al*., 2016), hence the similarity to typical pulse rates, while the SWs in this study appear to be related to the respiration rhythm. In addition, our observation of a much slower underlying ISW frequency ~0.02 Hz, points to an even more extensive endogenous component that we believe indicates metabolic integration or self-regulation during deeper levels of jhāna meditation. We suggest that this infraslow activity corresponds to the slow alternations seen in fMRI/BOLD imagery of subjects in the resting state (Grooms *et al*., 2017), and may represent a harmonic "beating" between other SW frequencies present, similar to Steyn-Ross *et al*.'s (2010) model for ultra-slow oscillations.

Returning to our methodology of relating EEG activity to Buddhist understandings of jhāna (section 2.1), we concluded that meditation spindles are a consequence of disruption to attention, and related to the early stages of developing jhāna. In the case of SWs, the startling intensity observed for some meditators leads us to interpret this intensity as related to the jhāna factor *pīti*, which, as described in section 2.1, heralds an increased energisation leading to the second rūpa jhāna, also allowing the subsequent development of the third and fourth jhānas. In this interpretation, those meditators in Table 1 showing both strong spindle and strong SW activity, would correspond to the stage of gradually developing experience of the first and second rūpa jhānas, while those subjects showing strong SWs with either no or weak spindle activity would be consolidating their experience of the second rūpa jhāna, and those where powerful SW activity dominates would be developing the second, third and fourth rūpa jhānas. The near absence of alpha activity in the plots in Figure 7, and our assertion that alpha activity is intimately part of the DCs, would then confirm that such subjects have successfully withdrawn into jhāna consciousness, with the associated development of a vertex ROI related to this.

3.3. SPIKE-WAVE AND SEIZURE-LIKE OR EPILEPTIFORM ACTIVITY

In addition to spindle and SW activity, the occurrence of spike-waves (S-Ws) is reminiscent of absence epilepsy (Sadleir *et al*., 2009); in addition, some subjects develop the ability to intentionally evoke intense states with clonic features similar to epilepsy. However, in both cases meditators remain fully conscious without discomfort.

3.3.1 Spike-Wave (S-W)Activity

To minimise confusion with SWs and higher frequency beta and gamma activity, a bandpass of 0.53-70/150 Hz was applied as noted in section 2.2. In Table 1, eight subjects (11 independent recordings) show episodes of S-Ws, mainly occipital; mostly brief, 3-12 secs duration, similar to bursts in absence epilepsy, apart from subject 26 who shows extended S-W activity over ~50 secs. For some subjects S-W bursts occur spontaneously, with meditators unaware of any specific change in their subjective experience. Some others develop S-Ws when deliberately arousing strong energisation, or *pīti*, the third jhāna factor (Introduction). Whilst S-Ws in absence epilepsy are characterised by a sharp initial spike, followed by a relatively smooth decay, those during meditation show reverberatory or harmonic structure between spikes, illustrated by the four examples in Figure 8.

bioRxiv preprint doi: https://doi.org/10.1101/407544; this version posted January 15, 2019. The copyright holder for this preprint (which was not certified by peer review) is the author/funder. All rights reserved. No reuse allowed without permission.

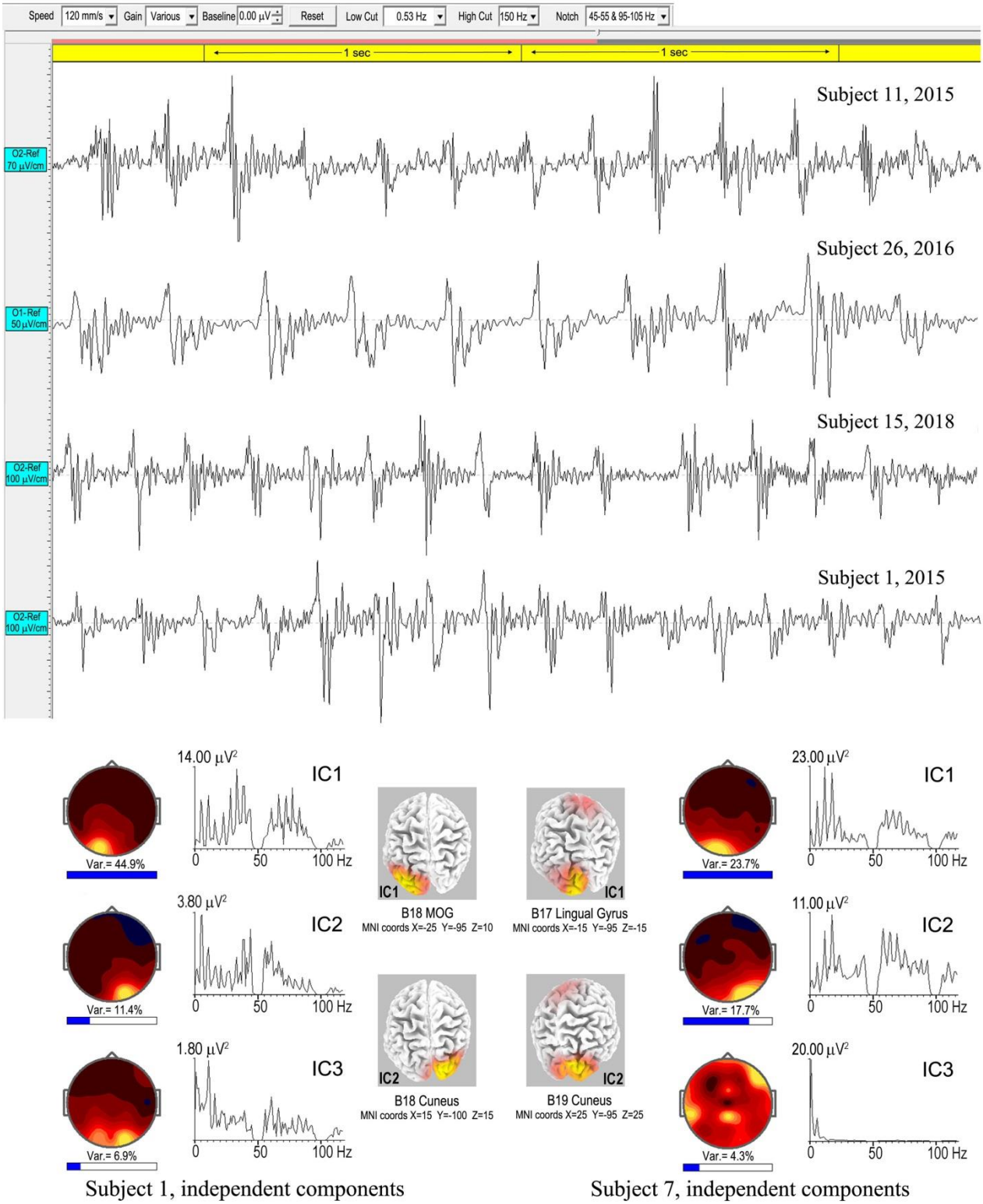

Figure 8 Examples of spike-wave (S-W) bursts at occipital sites O1 or O2. Top to bottom are excerpts from an 8.6-sec burst, subject 11, 2015; a 50-sec burst, subject 26, 2016; an 8.3-sec burst, subject 15, 2018; and a 3.025 sec burst, subject 1, 2015. Below are the strongest ICs for subjects 1 and 7, computed using eLoreta, showing harmonic spectral structure, spectral intensity distributions, and 3D source maps. The lower part of Figure 8 shows more detailed harmonic spectral structure from an eLoreta analysis for subjects 1 and 7, with spectral intensity distributions and 3D source maps.

Table 6 shows the results of an eLoreta source analysis of S-W segments from 9 independent records showing the clearest S-Ws (against background EEG).

bioRxiv preprint doi: https://doi.org/10.1101/407544; this version posted January 15, 2019. The copyright holder for this preprint (which was not certified by peer review) is the author/funder. All rights reserved. No reuse allowed without permission.

Subject year recorded	Spike-Waves (S-Ws)	B10 MFG (frontal lobe)	B11/B47 MFG SFG IFG (frontal lobe)	B6 MFG (frontal lobe)	B17/B18/B19 IOccG MOccG pCun Cun Ling (occipital lobe)	S-W spectral peaks from independent components
1. 2015	3.025 sec. segment At O1, O2, Oz 0.53-150 Hz 1-sec epochs				**35.5%** B19 MOccG -25 -95 10 **14.5%** B18 Cun 15 -100 15	5.37, 10.74, 16.13, 22.46, 28.32, 33.20, 38.58, 42.97,… 60.55, 66.41, 71.78, 77.15, 83.01
3. 2015	8.2 sec. segment At O1, O2, Oz 0.53-150 Hz 1-sec epochs		**7.1%** B11 MFG -10 65 -15		**23.8%** B17 Ling 20 -95 -5 **19.1%** B19 MOccG -40 -90 5	5.36, 10.74, 15.63 Hz
6. 2015	12.0 sec. segment At O1, O2, Oz 0.53-150 Hz 1-sec epochs	**7.9%** B10 MFG 10 65 0		**7.9%** B6 MFG 5 -30 70	**17.3%** B19 IOccG -40 -85 -10 **9.5%** B18 Cun 15 -100 0 **7.4%** B19 MOccG 45 -85 10	3.91, 7.81, 11.72, 15.63, 19.53, 23.44, 27.34, 31.25, 32.23, 36.13, 40.04, 43.95, ..72.27, 76.17, 80.08… Hz
7. 2015	7.0 sec. segment At O1, O2, Oz, Cz 0.53-150 Hz 1-sec epochs		**6.4%** B47 IFG -50 45 -10		**25.3%** B17 Ling -15 -95 -15 **18.3%** B19 Cun 25 -95 25	5.85, 11.72, 17.58, 23.44, 37.11, 41.99, 58.59, 64.45, 70.31, 76.17, 83.01, 85.94, 88.87, 92.77 … 105.47, 110.35 ….Hz
11. 2015	8.6 sec. segment At O1, O2, Oz 0.53-150 Hz 1-sec epochs				**22.2%** B18 Cun -25 -95 -5 **18.6%** B18 MOccG 20 -100 5 **9.2%** B19 MOccG -50 -80 0	4.88, 9.77, 14.65, 20.51, 25.39, 30.27, 38.09, … 59.57, 65.43, 69.34 ….. Hz
15 2016	10.6 sec. segment At O1, O2, Oz 0.53-70 Hz 1-sec epochs				**21.7%** B17 Ling -10 -95 -20 **21.1%** B18 IOccG 25 -90 -15 **7.2%** B18 Ling -5 -90 -20	7.81, 12.7, 15.63, 23.44, 30.27/31.25, 40.04,… Hz
15 2018	8.3 sec segment At O1, Oz, O2 0.53-150 Hz 1-sec epochs				**24.2%** B7 pCun 10 -80 40 **12.3%** B18 MOccG -5 -100 10 **9.7%** B18 Ling 0 -80 5 **3.8%** B19 IOccG 45 -85 -10	4.88/5.86, 10.74, 16.1, 21.48, 26.37, 28.32… 60.55, 66.41..Hz
24. 2016	5.0 sec. segment At O1, O2, Oz 0.53-70 Hz 1-sec epochs		**12.3%** B11 SFG 30 60 -10 **Slow wave cmpt**		**20.3%** B17 Cun 15 -90 5 **17.4%** B17 Ling -10 -95 -20	6.84, 10.74, 13.67, 21.48, 28.32, 35.16, 41.99 Hz
26. 2016	50.0 sec. segment At O1, O2, Oz 0.53-70 Hz 2-sec epochs		**9.4%** B47 IFG 50 45 -10 **Slow wave cmpt**		**29.7%** B18 Ling -20 -100 -10 **10.9%** B17 Ling 5 -95 -5	3.42, 6.84/7.32, 10.74, 14.16, 17.58, 21.00/21.48 Hz
Sub-Totals **Norm. to 100%**		**7.9%** **1.8%**	**35.2%** **7.8%**	**7.9%** **1.7%**	**399.0%** **88.7%**	
ROIs **Norm. to 100%**		**B10 B11 B47 Frontal** **9.6%**		**B6 Frontal near vertex** **1.7%**	**B17 B18 B19 Occipital** **88.7%**	

Table 6 Spike-Wave (S-W) sources from eLoreta for 9 independent records, 2015-18, bandpass 0.53-70/150 Hz, 1-sec epochs. MFG, SFG, IFG = medial, superior and inferior frontal gyri; IOccG, MOccG = inferior and middle occipital gyri; pCun, Cun, Ling = precuneus, cuneus and lingual gyrus. For each subject, the 3-6 strongest ICs were used that accounted for at least 50% of the signals' variance, then normalised to exactly 50% variance, for each subject. The final totals across all the recordings are normalised to 100%. An IC algorithm was used for subjects 3 and 11 to remove eye-blinks.

We find harmonic structure in all cases, with a range of spectral peaks for the strongest ICs shown in column 7, with harmonics underlined. Cortical sources computed as before using eLoreta, are in columns 3-6, with mean ROIs shown in the bottom row. Occipital sources overwhelmingly dominate at electrode sites O1, Oz and O2, accounting for 88.7% of the total signals' variance, with 9.6% and 1.7%

bioRxiv preprint doi: https://doi.org/10.1101/407544; this version posted January 15, 2019. The copyright holder for this preprint (which was not certified by peer review) is the author/funder. All rights reserved. No reuse allowed without permission.

frontal, and frontal-near-vertex, contributions respectively. Since some SW breakthrough remains in some cases, this occipital dominance is likely an underestimate. This occipital dominance is strikingly different to more widely varying locations, often frontal, in absence epilepsy (Stefan, 2013).

3.3.2. Seizure-Like or Epileptiform Activity

As noted in the Introduction, the transition from the first rūpa jhāna to the second and higher jhānas requires the meditator to become familiar with bodily energisation *pīti*. This typically develops in a natural way during Samatha meditation, but in the Yogāvacara tradition (as in Tibetan Buddhist yoga) there are specific techniques, involving breath control, to deliberately evoke high energy states. This is not a fixed requirement of the practice, but is undertaken by those with a special interest. The rationale is to become familiar not only with the ability to evoke higher energy states, but, more importantly, the ability to then tranquilize that energy back into a more intense experience of absorption (which we have suggested above is related to the high-energy SWs we observe). To an observer, the subject typically displays clonic features similar to epilepsy, but without discomfort, with the ability to evoke the state and leave it at will. Figure 9 shows two examples, taken from a wide range of presentations of this form of activity, analysis of which is at an early stage and may be the subject of a future paper. These examples are included to complete this overview and to illustrate some of the broad features.

Example A is from an experienced practitioner. The first sign of increasing energisation is the development of occipital S-Ws, followed immediately by a ~½sec global ictal burst, a second burst 3 secs later, another ~7 secs later, followed by the main body of the "seizure" 15 secs later. Physically, the meditator shows mild clonic jerks or bodily vibration, mostly along the vertical bodily axis. The expanded view below the top panel shows the occipital S-Ws, with a related and rather remarkable near-sinusoidal rhythm at the right temporal site T6, reaching p-p values ~3000 μV. To the right are the two strongest independent components (ICs) from an eLoreta analysis for the main 26-sec event, highlighted yellow. The activity is highly localised at Brodmann 37, MTG (MNI coordinates xyz 60 -60 -5), with S-W frequency 5.62 Hz, with the temporal activity at the harmonic, 11.23 Hz.

Example B is more complex, with stronger clonic activity. The EEG again shows brief global ictal bursts at the onset, shown in the expanded view below together with respiration. The ictal bursts coincide with the end of the out-breaths, and occipital S-Ws develop progressively rather than precede the "seizure" as in example A. Probably because of the complex mix of activity in this example, that includes very strong SW bursts, as well as occipital S-Ws and complex activity extending into the gamma band, a source analysis is inconclusive, returning a range of small sources rather than any one or two dominant sources. Strong SWs, as in this example, feature regularly in the more clonic examples of this activity, and we believe perform a containment function for the disturbance.

3.3.3 Discussion

Whilst epileptic S-W bursts were for many years described as "generalized", rather than focal, often frontal, recent work such as Ji *et al.*'s (2015) fMRI study, identifies specific thalamo-cortical networks showing increased connectivity during S-W bursts. These include prefrontal-thalamic, motor/premotor-thalamic, parietal/occipital-thalamic, and temporal-thalamic networks. Similarly, Chiosa *et al.* (2017), using dense-array EEG, find significant connectivity changes between thalamus to frontal sites, and from frontal and temporal sites to thalamus, preceding S-Ws. However, the S-Ws we observe are overwhelmingly occipital, indicating a different mechanism, as does the range of S-W frequencies and harmonic structure, rather than the typical 3.0-4.0 Hz focal frequency of epileptic S-Ws. As far as we are aware, there have been no reported findings of harmonic structure in the vast literature on epileptic S-Ws, which makes our findings all the more intriguing.

bioRxiv preprint doi: https://doi.org/10.1101/407544; this version posted January 15, 2019. The copyright holder for this preprint (which was not certified by peer review) is the author/funder. All rights reserved. No reuse allowed without permission.

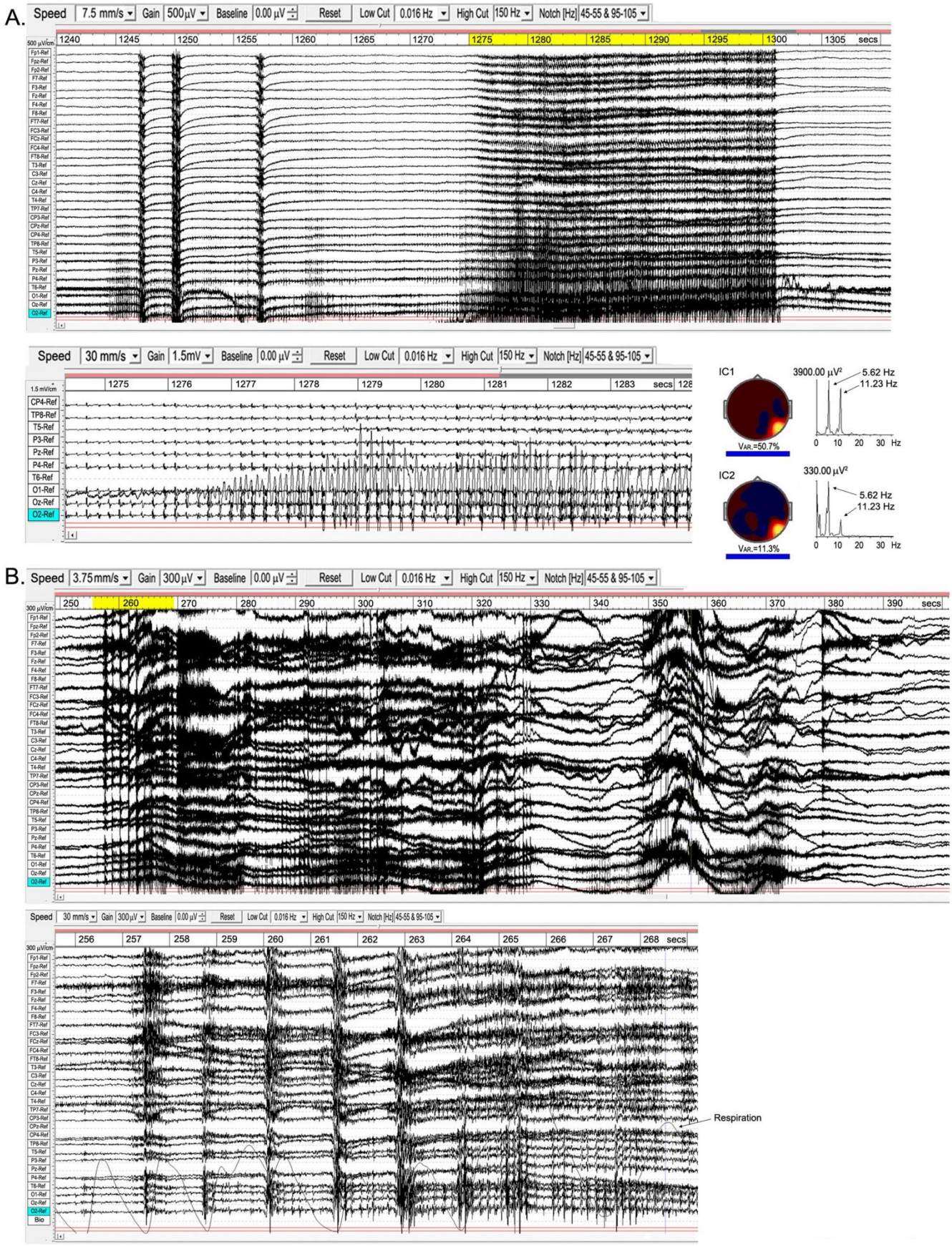

Figure 9 Examples of epileptiform activity. **A**, subject 15, 2018; the main 70-sec episode is shown in the top panel, with occipital activity expanded below. At right is a source analysis from the main body of the episode (yellow-highlighted). **B**, subject 7, 2015; the main 150-sec episode above, with an expanded view of the early part of the "seizure" (yellow-highlighted) below, together with respiration trace.

bioRxiv preprint doi: https://doi.org/10.1101/407544; this version posted January 15, 2019. The copyright holder for this preprint (which was not certified by peer review) is the author/funder. All rights reserved. No reuse allowed without permission.

The increased functional connectivity during epileptic S-W discharges is believed to reflect high levels of excitation and synchronization in one or more cortico-thalamic feedback loops, due to pathological conditions, locking the network(s) into fixed ~3.5 Hz oscillation. In meditation, however, intentional rather than pathological, we suggest the meditation S-Ws reflect a different form of destabilisation of the thalamo-cortical feedback loops when the personal element is withdrawn. And, further, because of the dominance of the occipital hub, that it is the "I/Eye" occipital-thalamic loop that is disrupted.

The intentionally evoked "seizure-like" activity, including S-Ws, presumably reflects the ability of some meditators to push the energisation inherent to jhāna meditation beyond a threshold into instability. What is intriguing is that these phenomena do not appear to overly disturb the meditator's tranquillity.

4. SUMMARY AND CONCLUDING DISCUSSION

We have approached this study by focusing on very specific EEG activity, not seen before, where the common factor is the practice of Buddhist jhāna meditation by subjects ranging from those with relatively early experience, to some with substantial experience. The detailed analysis of each of the observed themes in EEG activity, in the cross-discipline context of Buddhist understandings of jhāna, leads to intriguing insights into the nature of our default consciousness, and its intentional disruption, and the following summary and final discussion is presented as "informed hypotheses".

4.1. PROGRESSIVE WITHDRAWAL FROM THE DCs

Stage 1 Our discussion of spindling in this form of meditation strongly suggests it represents a disruption to attention, and, given the role of attention in jhāna meditation, is interpreted as an early sign of withdrawing attention from the DCs in the approach to jhāna and development of the first rūpa jhāna, as outlined in the Introduction. From the cortical source reconstruction and associated discussion, the results suggest disruption of the dorsal and ventral perception/attention streams that are, by definition, an integral part of the DCs networks. The meditational spindle frequencies, 7.5-10.5 Hz, are significantly lower than alpha spindles typical of attentional distraction within the DCs, such as driver distraction, and even lower still than those of sleep spindles, 10.0-14.0 Hz (Table 1). The range we find of 7.5-10.5 Hz corresponds well with the lower frequency ventral component of the alpha rhythm described by Barzegaran *et al*. (2017); which also corresponds to our finding significant limbic sources underlying meditation spindles.

We further speculate that the typical human peak alpha frequency ~9-11 Hz, and its close relationship to the mind-body reaction time ~100 ms, suggests that the alpha rhythm performs the key time-synchronizing role within DCs networks, and is biologically and evolutionarily favoured for optimal response to threat and for species survival. Those networks of the DCs (the NCC of current neuroscience) represent complex thalamo-cortical feedback loops, and we suggest that this network structure is the result of an *attractor* process towards a state of optimum metastability (Deco *et al*., 2017), corresponding to Friston's (2010) principle of minimisation of the brain's free energy, and characterised by the centrality of the alpha rhythm. This key role of the alpha rhythm then in turn can account for the scale structure of the α, β and γ bands in the DCs EEG, described by Palva and Palva (2007). The nature of the meditational spindles suggests that when the personal component is withdrawn from the cortico-thalamic feedback loops, the DCs is disrupted to the extent that the alpha *attractor* fails, and the feedback loop is unable to retain the alpha focus. We consider the possibility of other *attractor* modes in the following.

Stage 2 As described in section 1.2.2, as jhāna consciousness develops, a growing awareness and intensification of body-mind energies supporting that consciousness emerges in the form of the jhāna factor *pīti*, presaging the development of the second and (once *pīti* is mastered) higher rūpa jhānas. In terms of process, this would correspond to the unusually high energy states we observe for some meditators in their EEG.

bioRxiv preprint doi: https://doi.org/10.1101/407544; this version posted January 15, 2019. The copyright holder for this preprint (which was not certified by peer review) is the author/funder. All rights reserved. No reuse allowed without permission.

While the scalp EEG activity is intriguing – the near-annulus of excitation-inhibition from high-voltage SWs, with a developing region near the vertex – the source analysis reveals that the dominant cortical ROI is strongly at the vertex, bridging a midline area extending from B6, just frontal to the vertex, to parietal sites B5 and B7 just posterior to the vertex, accounting in total for 44.4% of total signals' variance across 8 independent records (Figure 6); with the next strongest ROIs frontal (24.2%), occipital (19.3%) and temporal (10.2%). These cortical "hubs" are interesting when considered against the nature of jhāna as progressively moving from a sensorily-determined subject-object basis of consciousness, towards the inner absorption common to all the jhānas and described by the jhāna factor *ekaggatācitta*, or one-pointedness of mind (sections 1.2.2, 1.2.3). On that basis, we suggest that the occipital and frontal hubs represent the residual subject and object poles, respectively, of the sensory DCs, the temporal contribution the residual part of the ventral perceptual stream, while the vertex hub is a sign of the emerging second rūpa jhāna consciousness. In this model, the occipital hub, integral to the dorsal and ventral perceptual streams of the DCs, carries the first-person "I/eye" pole of sensory consciousness (Merker 2013); while the frontal hub, well researched as part of the executive attention network, carries the object pole due to its role in cognitive processing (Petersen and Posner, 2012).

The vertex sites, B6, B5 and B7 include the supplementary motor area (SMA), strongly connected to the thalamus and projecting directly to the spinal cord, and the highly connected medial parietal associative cortex, believed to be involved in a wide variety of high-level processing tasks, with dense links to the underlying cingulate, thalamus and brain stem. This vertical-axis connectivity is striking in contrast to the (suggested) front-back axis of the DCs, and suggests involvement of the ascending reticular activating system (ARAS), with its known involvement in arousal, attention and consciousness (Maldonato, 2014). It is known that disruptions to the ARAS can lead to coma (Norton, 2012), and disruption of posterior cingulate connectivity can cause unconsciousness (Herbet, 2014), but the form of disruption we see in this form of meditation does not lead to unconsciousness, even though the strong SWs have superficial similarities to deep sleep and coma, as discussed earlier.

Stage 3 As noted in section 1.2.3, the third rūpa jhāna is described as "completely conscious" in the 5th-century *Vimuttimagga*, which quality is continued into the fourth rūpa jhāna, the two being essentially very similar except that the fourth no longer depends on the "reward" of happiness or pleasure to sustain equanimity. It might therefore be expected that the frontal and occipital residuals of the DCs described above might finally disappear during progression from the second to the third and fourth jhānas. The recordings of subject 5 in 2014 and 2017 appear to confirm this, showing as they do an almost complete dominance of vertex sources, particularly in 2017 (Table 5) when this subject had considerably more experience of jhāna meditation. Vertex activity became highly focused at an astonishing 99.7%, with only tiny residual frontal and occipital contributions of 0.2% and 0.1% respectively (Figure 7). An examination of all 31 ICs showed the vertex sources to be almost entirely represented by high-voltage SWs, against background broadband gamma activity and tiny residual alpha components (Figure 7). Implications of this remarkable focus are discussed below.

4.2. CONSCIOUSNESS

To date, research on the NCC has been limited to the DCs, the human default sensory consciousness. This DCs is supported by a highly complex set of cortical networks in dynamic equilibrium to minimise free energy (Friston, 2010), with the personal component necessarily taking a central role. It should therefore be no surprise that task-based studies reveal a sometimes bewildering array of NCC networks supporting the DCs. There is growing convergence of evidence, which our study supports, that the temporal scale factor for the DCs is the alpha frequency, linked as it is to a minimum processing time from sensory input, through cognitive processing and evaluation as to significance to the "self", to decision and action involving the body via the sensory-motor and motor systems of the brain. The EEG frequency bands δ, θ, α, β and γ then become expressions of that scale factor, each independent and carrying different functions, but highly interconnected as postulated by Klimesch (2013). In terms of different functions, it might be said that α activity characterises a minimum processing time for

bioRxiv preprint doi: https://doi.org/10.1101/407544; this version posted January 15, 2019. The copyright holder for this preprint (which was not certified by peer review) is the author/funder. All rights reserved. No reuse allowed without permission.

perception to action (a conscious "thought"); β the underling faster unconscious cognitive processes; θ the slower function of bridging more than one α process, facilitating memory; and γ higher-level functions perhaps related to consciousness of the whole.

As meditators withdraw attention from the DCs, the first disruptions we observe are to the dorsal and ventral perceptual attention streams. The alpha attractor begins to fail, evidenced by the nature of the spindles we see. As withdrawal deepens, and powerful SWs develop, the active cortical networks simplify to near-midline frontal and occipital ROIs, and an increasingly strong, and eventually dominant vertex ROI (Figure 6), with θ, α and β activity typical of the DCs now virtually absent, leaving only broadband gamma activity in the background. We suggest therefore that attention processes constitute the "outer" cognitive shell of the DCs, and that the more personal subject-object nature of the DCs is carried by reciprocal occipital-frontal (respectively) cortical networks that are progressively disrupted as jhāna consciousness develops. The point that consciousness has to have an object is sometimes overlooked in the literature, and certainly for the DCs it is unrealistic to imagine the NCC could be located in a single region, such as the front or back of the head, rather than through reciprocal connectivity.

Both in textual description and as subjectively experienced, the jhānas are regarded as states of consciousness, with the object of each jhāna becoming increasingly more subtle. From our study, jhāna consciousness appears to be characterised by the scale factor of the respiration cycle, with the SW periodicity (Table 4; 8.36±0.60 secs, or 0.125±0.010 Hz) very close to that of respiration; not entirely a surprise given that the breath is the primary object in the early stages. However, as a scale factor this is almost two orders of magnitude slower than the 100 ms of the DCs, which might explain the expanded sense of time and spaciousness meditators describe during this form of meditation, and the frequent rendering of Samatha as undisturbed peace or tranquillity.

The development of a vertex-body axis, rather than the frontal-occipital axis of the DCs, and evidence of an underlying ISW activity ~0.02 Hz, suggests an even slower metabolic scale factor integrating the entire mind-body system in the deeper levels of jhāna. The intense vertex focus, unlike the dual frontal-occipital ROIs of the DCs, raises the interesting question as to what is the nature of the subject-object structure of jhāna consciousness, since an object is still required to be *conscious of*. In the oral jhāna tradition, several views are expressed. One is that each moment of consciousness becomes the object of the next, giving the illusion of perfectly still and continuous undisturbed consciousness. This is envisaged as a high level and very fast process, and we might wonder at the role of the background gamma activity and brief gamma bursts we frequently observe. A second view is that the body itself is the supporting object of jhāna consciousness, as part of a deep metabolic integration, and perhaps related to the intriguing term "body witness" sometimes encountered in the ancient texts (e.g. *Vimuttimagga*).

In nREM sleep, the scale factor is the heart rhythm (Mensen, 2016), with corresponding SW frequencies ~1.0-1.2 Hz. However, the fact that SW nREM sleep is unconscious, unlike either the DCs, or jhāna consciousness also characterised by SW activity, raises the intriguing question as to what is different in cardio-cortical connectivity during nREM sleep, that leads to a disconnect from sensory and motor networks in the absence of any intense stimulus to cause awakening. And what is the purpose of the disconnect?

4.2.1. Harmonic structure

The meditation spike-waves (S-Ws), either involuntary or as part of deliberately enhancing energisation beyond a threshold of instability, all show harmonic spectral structure, unlike those in epileptic or pathological states, and do not disturb meditators' conscious experience. Their specific occipital location around the lingual, cuneal and occipital gyri suggests disruption to the "I/Eye" component of consciousness, and therefore the occipito-thalamic feedback network. We believe this is additional evidence of disruption to the δ, θ, α, β scaled activity of the DCs, and that the harmonic structure is

bioRxiv preprint doi: https://doi.org/10.1101/407544; this version posted January 15, 2019. The copyright holder for this preprint (which was not certified by peer review) is the author/funder. All rights reserved. No reuse allowed without permission.

evidence that withdrawal of the personal "I" component from the occipito-thalamic network triggers the thalamus into harmonic activity in an attempt to stimulate scaled network activity similar to that of the DCs. The implication is that harmonic or fractal structure is an integral part of thalamo-cortical network connectivity, and that the δ, θ, α, β structure of the DCs is but one example, that we presume is optimal for sensory consciousness and minimisation of free energy.

4.3. ENERGY AND STABILITY

Several of our examples exhibit SW amplitudes >2000 μV p-p, compared to typical EEG resting-state values 25-45 μV p-p. Also, in some cases SWs develop very rapidly following the cue to start meditation, as in the lower panels of Figures 3 and 4, showing high cortical responsiveness. A striking example is subject 5 (2017), where signal amplitude at the vertex site Cz increased from ~25-30 μV p-p before SW onset, to an initial de-excitation reaching -2630 μV p-p, followed by a recovery to the familiar pattern of alternating excitation/de-excitation at ~400-2000 μV p-p for the next 20 mins. The initial voltage ratio ~95, corresponds to a power ratio >9000, almost 4 orders of magnitude. The strongest individual SWs, as in the middle panel of Figure 3, show a rapid rise as high as 1100-1300 μV/s, followed by a much slower over-shooting decay, similar to that of a relaxation oscillator.

The corresponding subjective experience during these high-energy states is one of deep equanimity, and as several subjects describe, a sense of vivid presence, rather than instability or disturbance. In the case of those subjects that show occipital S-Ws, they also are not aware of any disturbance, other than mild enhanced energisation. And for those who are able to intentionally evoke clonic epileptiform states (Figure 9), they do so with no discomfort, are able to control the duration and to leave the state when they choose, quickly recovering composure and equanimity. The comparison to epileptic states is nevertheless intriguing, and example 1 from Figure 9 may add another piece to the puzzle. In this example, strong occipital S-Ws appear to trigger an exceptionally strong resonance (reaching 3000 μV p-p) in the right middle-temporal gyrus, at the first harmonic of the S-W frequency. What lies behind the sensitivity of the temporal gyrus, a frequent site of pathological seizures, to be destabilised in this way?

We believe that the capacity to manage and contain high-energy states is the result of the detailed development of attention, often over many years, coupled with the deliberate use of non-normal lengths of breath as noted in the Introduction. Over 50 years, and with currently over 400 practitioners, this particular practice has proved remarkably safe, and we wonder whether some of the basic features of its attentional development could be adapted for epilepsy sufferers with the goal of reducing frequency of seizures.

Finally, while recent neuroscience has explored in depth the minimisation of free energy as a key factor in the brain's default energy balance, this study highlights that disruption of the DCs reveals a hitherto unrecognised and remarkable reservoir of *available* energy. It also demonstrates an equally remarkable *responsiveness* of the brain's cortical networks during this form of meditation, which we presume is related in some way to the more common focus on plasticity.

4.5. CONFLICTS OF INTEREST

This research has been conducted in the absence of any commercial or financial relationships that could be construed as a potential conflict of interest.

ACKNOWLEDGEMENTS

We are grateful for the willing cooperation of all the subjects who participated in this study, and the ethical approval granted by The Samatha Trust.

REFERENCES

bioRxiv preprint doi: https://doi.org/10.1101/407544; this version posted January 15, 2019. The copyright holder for this preprint (which was not certified by peer review) is the author/funder. All rights reserved. No reuse allowed without permission.

American Academy of Sleep Medicine (AASM) (2017) The AASM manual for the scoring of sleep and associated events: rules, terminology and technical specifications. https://aasm.org/clinical-resources/scoring-manual/

Barzegaran, E., Vildavski, V.Y. and Knyazeva, M.G. (2017) Fine structure of posterior alpha rhythm, in human EEG: frequency components, their cortical sources and temporal behaviour. *Scientific Reports*, **7**(8249). doi: 10.1038/s41598-017-08421-z

Bersaglieri, A., Pascual-Marqui. R.D., Tarokh, L. and Achermann, P. (2018) Mapping slow waves by EEG topography and source localization: effects of sleep deprivation. *Brain Topogr*. **31**(2), 257-69. doi: 10.1007/s10548-017-0595-6

Bizot, F. (1994, ed.) Recherches nouvelles sur le Cambodge. Paris: Ecole Francaise d'Extreme-Orient, 101-27.

Boly, M., Massimini, M., Tsuchiya, N., Postle, B.R., Koch, C. and Tononi, G. (2017) Are the neural correlates of consciousness in the front or in the back of the cerebral cortex? Clinical and neuroimaging evidence. *J. Neurosci.*, **37**(40), 9603-13. doi: 10.1523/jneurosci.3218-16

Buddhaghosa (5th century) *The Path of Purification: Visuddhimagga*. Kandy, Sri Lanka: Buddhist Publication Society, 2011.

Cahn, B.R. and Polich, J. (2006) Meditation states and traits: EEG, ERP, and neuroimaging studies. Psycholgical Bull. **132**(2), 180-211. doi: 10.3389/fpsyt.2014.00074

Chiosa, V., Groppa, S., Ciolac, D., Koirala, N., Misina, L., Winter, Y., Moldovanu, M., Muthuraman, M. and Groppa, S. (2017) Breakdown of thalamo-cortical connectivity precedes spike generation in focal epilepsies. *Brain Conn*., **7**(5).
doi: 10.1089/brain.2017.0487

Cloutman, L.L. (2012) Interaction between dorsal and ventral processing streams: where, when and how? *Brain & Language*, **127**, 251-63. doi: 10.2016/j.bandl.2012.08.003

Cousins, L.S. (1973) Buddhist jhāna: its nature and attainment according to Pali sources. *Religion* **3**, 115-131.

Cousins, L.S. (1994-96) The origin of insight meditation. *The Buddhist Forum, **IV**, Seminar Papers*, ed. Skorupski. London: Institute of Buddhist Studies.

Crosby,K. (2000) Tantric Theravāda: a bibliographic essay on the writings of Françoise Bizot and others on the Yogāvacara tradition. *Contemporary Buddhism*, **1(2)**.

Crosby, K. (2013) Traditional Theravāda Meditation and its Modern-Era Suppression. Hong Kong: Buddhist Dhamma Centre of Hong Kong.

Deco, G., Kringelbach, M.L., Jirsa, V.K. and Ritter, P. (2017) The dynamics of resting fluctuations in the brain: metastability and its dynamical cortical core. *Scientific Rep.*, **7**(3095). doi: 10.1038/s41598-017-03073-5

Del Felice, A., Arcaro, C., Storti, S.F., Fiaschi, A. and Manganotti, P. (2014) Electrical source imaging of sleep spindles. *Clin. EEG and Neurosci*., **45**(3), 184-92.
doi: 10.1177/1550059413497716

Delorme, A. and Makeig, S. (2004) EEGLAB: an open source toolbox for analysis of single-trial EEG dynamics including independent component analysis. *J. Neurosci. Methods*, **134**, 9-21. doi: 10.1016/j.neumeth.2003.10.009

Dennison,P. (2012) Quantum mind, meditation and brain science. *Paendim Dhamma Foundation*. Bangkok: Sangsilp Press.

Foxe, J.J. and Snyder, A.C. (2011) The role of alpha-band brain oscillations as a sensory suppression mechanism during selective attention. *Front. Psych*., **2**(154). doi: 10.3389/fpsyg.2011.00154

Freud, S. (1895) Project for a Scientific Psychology. Standard Edition, Vol. 1. London: Hogarth Press.

Friston, K. (2010) The free-energy principle: a unified brain theory? *Nature Revs Neurosci*., **11**, 127-39. doi: 10.1038/nrn2787

Friston, K, FitzGerald, T., Rigoli, F., Schwartenbeck, P., O'Docherty, J. and Pezzulo, G. (2016) Active inference and learning. *Neurosci. & Biobehav. Revs*. **68**, 862-79.
doi:10.1016/j.neubiorev.2016.06.022

Gent, T. and Adamantidis, A. (2017) Anaesthesia and sleep: where are we now? *Clin. & Translat. Neurosci.*, **1**(1). doi: 10.1177/2514183X17726281

bioRxiv preprint doi: https://doi.org/10.1101/407544; this version posted January 15, 2019. The copyright holder for this preprint (which was not certified by peer review) is the author/funder. All rights reserved. No reuse allowed without permission.

Grandy, T.H., Werkle-Bergner, M., Chicherio, C., Schmiedek, F., Lovden, M. and Lindenberger, U. (2013) Peak individual alpha frequency qualifies as a stable neurophysiological trait marker in healthy younger and older adults. *Psychphysiology*, **50**, 570-82. doi: 10.1111/psyp.12043

Grooms, J.K., Thompson, G., Pan, W.-J., Billings, J., Schumacher, E.H., Epstein, C.M. and Keilholz, S.D. (2017) Infraslow EEG and dynamic resting state network activity. *Brain Conn.*, **7**(5). doi: 10.1089/brain.2017.0492

Gunaratana, H. (1980) A Critical Analysis of the jhānas in Theravada Buddhist meditation. PhD dissertation. Washington: The American University.

Hagerty, M.R. *et al.* (2013) Case study of ecstatic meditation: fMRI and EEG evidence of self-stimulating a reward system. *Neural Plasticity*, **3**. doi: 10.1155/2013/653572

Hagihira, S. (2017) Brain mechanisms during course of anesthesia: what we know from EEG changes during induction and recovery. *Front. Sys. Neurosci.* **11**(39). doi: 10.3389/fnsys.2017.00039

Herbet, G., Lafargue, G., Menjot de Champfleur, N., Moritz-Gasser, S., le Bars, E., Bonnetblanc, F. and Duffau, H. (2014) Disrupting posterior cingulate connectivity disconnects consciousness from the external environment. *Neuropsychologia*, **56**, 239-44. doi: 10.1016/j.neuropsychologia.2014.01.020

Hight, D., Voss, L.J., Garcia, P.S. and Sleigh, J. (2017) Changes in alpha frequency and power in the electroencephalogram during volatile-based general anesthesia. *Front. Sys. Neurosci.*, **11**(36). doi: 10.3389/fnsys.2017.00036

Hohwy, J. (2009) The neural correlates of consciousness: new experimental approaches needed? Consciousness & Cogn. **18**(2), 428-438. doi: 10.1016/j.concog.2009.02.006

Hohwy, J. (2012) Attention and conscious perception in the hypothesis testing brain. *Front. Psych.*, **3**(96). doi: 10.3389/fpsyg.2012.00096

Jensen, O. and Mazaheri, A. (2010) Shaping functional architecture by oscillatory alpha activity: gating by inhibition. *Human Neuroscience*, **4**(186). doi: 10.3389/fnhum.2010.00186

Joshi, C. N. and Patrick, J. (2007) Eyelid myoclonia with absences: routine EEG is sufficient to make a diagnosis. *Seizure*, **16**, 254-60. doi: 10.1016/j.seizure.2007.01.003

Klimesch, W. (2013) An algorithm for the frequency architecture of consciousness and brain body coupling. *Front. Hum. Neurosci*., **7**(766). doi: 10.3389/fnhum.2013.00766

Koch, C., Massimini, M., Boly, M. and Tononi, G. (2016) Neural correlates of consciousness: progress and problems. *Nature Rev. Neurosci*. **17**, 307-21. doi: 10.1038/nrn.2016.61

Kravitz, D.J., Saleem, K.S., Baker, C.I. and Mishkin, M. (2011) A new neural framework for visuospatial processing. *Nat. Rev. Neurosci.*, **12**(4), 217-30. doi: 10.1038/nrn3008

Leresche, N., Lambert, R.C., Errington, A.C. and Crunelli, V. (2012) From sleep spindles of natural sleep to spike and wave discharges of typical absence seizures: is the hypothesis still valid? *Eur. J. Physiol.*, **463**, 201-12. doi: 10.1007/s00424-011-1009-3

Libenson, M.H. (2012) Practical Approaches to Electroencephalography, Ch. 12 "EEG patterns in stupor and coma". Saunders Elsevier Press.

Maldonato, N.M. (2014) "The ascending reticular activating system: the common root of consciousness and attention", in Recent Advances of Neural Network Models and Applications, *Proc. 23rd Workshop Italian Neural Networks Soc.* doi: 10.1007/978-3-319-04129-2_33

Massimini, M., Huber, R., Ferrarelli, F., Hill, S. and Tononi, G. (2004) The sleep slow oscillation as a travelling wave. *J. Neurosci*. **24**(31), 6862-70. doi: 10.1523/jneurosci.1318-04.2004

Matte Blanco, I. (1980) The unconscious as infinite sets: an essay in bi-logic. London: Karnac.

Mensen, A., Zhang, Z., Qi, M. and Khatami, R. (2016) The occurrence of individual slow waves in sleep is predicted by heart rate. *Scient. Repts*. **6,** doi:10.1038/srep29671 (2016).

Merker, B.H. (2013) The efference cascade, consciousness, and the self: naturalizing the first person pivot of action control. *Front. Psychol*. **4**(501). doi: 10.3389/fpsyg.2013.00501

Milner, A.D. (2017) How do the two visual streams interact with each other? *Exp. Brain Res.* **235**(5),1297-1308. doi: 10.1007/s00221-017-4917-4

Minvaleev, R.S., Bogdanov, A.R., Bogdanov, R.R., Bahner, D.P. and Marik, P.E. (2014) Hemodynamic observations of Tumo yoga practitioners in a Himalayan environment. *J. Alt. & Compl. Med.*, **20**(4), 295-99. doi: 10.1089/acm.2013.0159

bioRxiv preprint doi: https://doi.org/10.1101/407544; this version posted January 15, 2019. The copyright holder for this preprint (which was not certified by peer review) is the author/funder. All rights reserved. No reuse allowed without permission.

Mitsar Medical. http://www.mitsar-medical.com/

Murphy, M. *et al*. (2009) Source modelling sleep slow waves. *Proc. Natl Acad. Sci*. *USA* **106**(5), 1608-13. doi: 10.1073/pnas.0807933106

Nagara Sutta, Samyutta Nikaya 12.65. Trans. Bhikkhu Bodhi, 2000. Somerville MA: Wisdom Publications.

Norton, L., Hutchison, R.M., Young, G.B., Sharp, M.D. and Mirsattari, S.M. (2012) Disruptions of functional connectivity in the default mode network of comatose patients. *Neurology* **78**(3),175-81. doi: 10.1012/WNL.0b013e31823fcd61

Palva, S. and Palva, J.M. (2007) New vistas for α-frequency band oscillations. *Trends Neurosci*., **30**(4), 150-8. doi: 10.1016/j.tins.2007.02.001

Pascual-Marqui, R.D. (2002) Standardized low resolution brain electromagnetic tomography (sLoreta): technical details. *Methods & Findings Exp. Clin. Pharmacol*. **24D**, 5-12.

Pascual-Marqui, R.D. (2007) Discrete, 3D distributed, linear imaging methods of electric neuronal activity. Part 1: exact, zero error localization. *arXiv:0710.3341 [math-ph]*, http://arxiv.org/pdf/0710.3341.

Petersen, S.E. and Posner, M.I. (2012) The attention system of the brain: 20 years after. *Annu. Rev. Neurosci*. **35**, 73-89. doi: 10.1146/annurev-neuro-062111-150-525

Purcell, S.M., Manoach, D.S., Demanuele, C., Cade, B.E., Mariani, S., Cox, R. *et al.* (2017) Characterizing sleep spindles in 11,630 individuals from the National Sleep Research Resource. *Nat. Comm.*, **8**(15930). doi: 10.1038/ncomms15930

Raichle, M.E. (2015a) The brain's default mode network. *Ann. Rev. Neurosci.*, **38**, 433-47. doi: 10.1146/annurev-neuro-071013-014030

Raichle, M.E. (2015b) The restless brain: how intrinsic activity organizes brain function. *Phil. Trans. R. Soc. B* **370**, 20140172. doi: 10.1098/rstb.2014.0172

Ryle, A. and Kerr, I.B. (2002) Introducing Cognitive Analytic Therapy: Principles and Practice. London: Wiley.

Sadleir, L.G., Scheffer, I.E., Smith, S., Carstensen, B., Farrell, K. and Connolly, M.B. (2009) EEG features of absence seizures in idiopathic generalized epilepsy: impact of syndrome, age and state. *Epilepsia*, **50**(6), 1572-8. doi: 10.1111/j.1528-1167.2008.02001.x

Sitaram R, Ros T, Stoeckel L, Haller S, Scharnowski F, Lewis-Peacock J, et al. (2017) Closed-loop brain training: the science of neurofeedback. *Nature Reviews Neuroscience*. **18**(2),86-100. doi: 10.1038/nrn.2016.164 PMID: 28003656

Sonnleitner, A., Simon, M., Kincses, W.E., Buchner, A. and Schrauf, M. (2012) Alpha spindles as neurophysiological correlates indicating attentional shift in a simulated driving task. *International Journal of Psychophysiology*, **83**, 110-18. doi: 10.1016/j.ijpsycho.2011.10.013

Souza, R.T.Fd., Gerhardt, G.J.L., Schönwald, S.V., Rybarczyk-Filho, J.L. and Lemke, N. (2016) Synchronization and propagation of global sleep spindles. *PLoS One* **11**(3): e0151369. doi:10.1371/

Stefan, H. and Lopez da Silva, F.H. (2013) Epileptic neuronal networks: methods of identification and clinical relevance. *Front. Neurol.*, **4**(8), 1. doi: 10.3389/fneur.2013.00008

Steyn-Ross, M.L., Steyn-Ross, D.A., Sleigh, J.W. and Wilson, M.T. (2011) A mechanism for ultra-slow oscillations in the cortical default network. *Bull. Math. Biol*., **73**, 398-416. doi: 10.1007/s11538-010-9565-9

Sutter, R. and Kaplan, P.W. (2012) Electroencephalographic patterns in coma: when things slow down. *Epileptologie*, **29**, 201-9.

The Samatha Trust, regd UK Charity no. 266367 (1974). www.Samatha.org

The Yogāvachara's Manual (C17 th-18th). Trans F.M. Woodward, Pali Text Society (1916). London: Oxford University Press.

Thomas, J.W. and Cohen, M. (2014) A methodological review of meditation research. *Front. Psychiatry* **5**(74). doi: 10.3389/fpsyt.2014.00074

Upatissa Thera (~5th century) *The Path of Freedom: Vimuttimagga*. Maharagama, Sri Lanka: The Saman Press, 1961.

bioRxiv preprint doi: https://doi.org/10.1101/407544; this version posted January 15, 2019. The copyright holder for this preprint (which was not certified by peer review) is the author/funder. All rights reserved. No reuse allowed without permission.

Wallace, B.A. (1999) The Buddhist tradition of Samatha: methods for refining and examining consciousness. *J. Consciousness Studies*, **6**(2-3), 175-87.

Werth, E., Achermann, P., Dijk, D.-J., Borbely, A.A. (1997) Spindle frequency activity in the sleep EEG: individual differences and topographic distribution. *EEG and Clin. Neurophys.*, **103**(5), 535-42. doi: 10.1016/S0013-4694(97)00070-9

Ji, G.-J., Zhang, Z., Xu, Q., Wang, Z., Wang, J., Jiao, Q., Yang, F., Tan, Q., Chen, G., Zang, Y.-F., Liao, W. and Lu, G. (2015) Identifying cortico-thalamic network epicentres in patients with idiopathic generalized epilepsy. *Amer. J. Neuroradiol.* **36**(8). doi: 10.3174/ajnr.A4308